Bachelor's thesis

NTNU
Norwegian University of Science and Technology

Garshol, Askh
Hannah, Skarsvåg

Recycling of industrial silicon-kerf waste via leaching and flux-melting

Bachelor's thesis in Materials Science and Engineering
Supervisor: Safarian, Jafar
Co-supervisor: Mubaiwa, Tinotenda and Zhu, Mengyi
May 2023

NTNU
Norwegian University of
Science and Technology

Garshol, Askh
Hannah, Skarsvåg

Recycling of industrial silicon-kerf waste via leaching and flux-melting

Bachelor's thesis in Materials Science and Engineering
Supervisor: Safarian, Jafar
Co-supervisor: Mubaiwa, Tinotenda and Zhu, Mengyi
May 2023

Norwegian University of Science and Technology

NTNU
Norwegian University of
Science and Technology

Acknowledgements

While this thesis was worked on as a group and Hannah Skarsvåg is a co-author, this report was written by me, Askh Garshol. This past semester would not have been possible to complete without the assistance and full support of my supervisors, teachers, department engineers and my friends and family. First of all, I would like to thank Jafar Safarian, Tinotenda Mubaiwa and Mengyi Zhu who were my supervisors, for all the help and support they offered the past semester. I would also like to thank Dmitry Slizovskiy, Andrey Kosinskiy, Sergey Khromov and Ruben Hansen who were department engineers who assisted in the lab work by teaching me how to use the different instruments and techniques used in the experimental work. Last but not least, I would like to thank my friends and family who during this semester provided me with the support needed to carry out my work.

Abstract

The production of solar grade silicon wafers used in solar cell production is a long and complex process that results in 50% of pure silicon being wasted. This volume of waste has been a problem that has impacted the industry for many years now and different methods of recycling have been brought forward and patented to try and combat this high volume of silicon waste. REC Solar Norway is a pioneer when it comes to different process and methods used to produce silicon as the ELKEM process. The purpose of this research and lab work was to use silicon kerf from industry waste and remove the impurities within the silicon kerf through pyrometallurgical and hydrometallurgical treatments and produce solar grade silicon. Acid leaching was used as the first step in the refinement process to remove metallic impurities while an induction furnace was used to melt the silicon kerf after leaching and to further remove impurities that the acid leaching could not remove. Two samples were melted without any additives while other samples were melted along $CaO\text{-}SiO_2$ slag and FBR Si. The characterization and analysis of the samples were carried out using electron microscopy and mass spectroscopy. The results from the refinement process were very promising and aligned with the theoretical aspects of this experiment. The GD-MS results pointed towards solar grade silicon being produced however an additional refinement step such as directional melting is needed, as well as further optimizing the leaching and melting process in order to produce solar grade silicon.

Sammendrag

Produksjonen av solar grade silisium oblater som brukes i solcelleproduksjon er en lang og kompleks prosess som resultater i at 50% av rent silisium blir kastet vekk etter kutte prossesen. Dette har vært et problem som har påvirket og plaget industrien i mange år, og ulike metoder og patenter for resirkulering har blitt fremmet for å prøve å bekjempe dette. REC Solar Norway er en bedrift som har kommet opp med ulike prosesser og metoder som brukes for å produsere silisum, som for eksempel ELKEM prosessen. Formålet med forskningen og laboratoriearbeidet var å bruke silisiumkerf fra indsutriavfallet og for å fjerne de ulike urenheter gjennom pyrometallurgiske og hydrometallurgiske behandlinger for å produsere solar grade siliusium. Syreutlutning var den første trinnet i foredlingsprossessen for å fjerne metalliske urenheter mens en induksjonsovn ble brukt til å smelte silisiumkerfen etter utluting og for å fjerne urenhter som ble ikke fjernet i utlutnings prossesen. To prøver ble smeltet uten tilsetningstoffer mens de andre prøvene ble smeltet sammen med CaO-SiO2 slag og FBR Si. Karakteriseringen og analysen av prøvene ble utført ved bruk av elektronmikroskopi og massespektroskopi. I samsvar med de teoretiske aspektene ved dette forsøket, var resultatene veldig lovende. GD-MS resultatene pekte imot at det ble produsert solar grade silisium, men et ekstra foredlingstrinn som direction solidification er nødvendig, samt ytterligere optimalisering av utlutnings og smelte prossesen for å produsere solar grade silisium.

Table of contents

1. Introduction

1.1 Background

The globe is experiencing growth all over the world in every sector and it is no different for the energy sector as well. As the energy sector grows, so will its demand and by 2050 experts predict that the global energy demand will grow by 47% [1]. Solar power has become a growing force within the renewable energy sector and experienced the second largest generation growth of all renewable technologies in 2021 [2]. Solar grade silicon (SoG-Si) is the material of choice when it comes to producing solar panels as energy into electrical power in an efficient manner. SoG-Si can be produced in several ways; however, the metallurgical method is the most cost effective and environmentally friendly method. SoG-Si suffers a major loss of value during the early stages of the manufacturing process. Silicon wafers that are used for solar cells are produced by cutting silicon ingots into very thin slices called wafers. It is during this process that up to 50% of the high purity silicon is discarded as waste [3]. This silicon waste is known as kerf, and it is usually disposed of due to the difficulty and time it takes to separate the silicon from the impurities. Landfills are usually used in the disposal of this silicon waste as the recycling of silicon is challenging. There are few methods that been reported and patented, however there are new technologies that are emerging, such as REC Solar Norway's new recycling process that aims to reduce the loss during the cutting and wafering process [4].

1.2 Aim of work

In this bachelor thesis, the main objectives are:

- The removal of impurities within the silicon kerf material through a combination of different methods. Pyrometallurgical and hydrometallurgical treatments will be carried out with the aim of producing SoG-Si.
- To evaluate the use of high temperature induction melting process on Si kerf, and the effect of slag and pure silicon additions on melting.
- Characterizing the materials using electron microscopy, mass spectroscopy and wet chemical methods and outline the possible methods that can be further used.
- To develop a sustainable process with low carbon dioxide (CO_2) emissions to recycle silicon from Si-kerf waste and improve upon the existing processes with higher silicon yields.

2. Theoretical background

2.1 Solar grade silicon production

2.1.1 Silicon

Silicon is an important element and has many applications worldwide. It's used in the steel industry, chemical industry and in the electronics industry. However, silicon is also an extremely important material used in the photovoltaic industry. There is a large abundance of silicon as it is a widely available material. After oxygen, silicon is the second most common element found on earth [5]. Silicon can be found within earth's crust in the form of soil, sand, and rocks such as obsidian, granite, and sandstone. Silicon is also a semiconductor material.

When silicon is exposed to light, the silicon absorbs the light photons and transfers the photons into electrons. The electrons then flow through the silicon as an electrical current and this current can then be extracted and used for solar panels [6]. This makes silicon a very cost-effective material for solar cell production while still being efficient enough at converting sunlight into usable electricity. As well as being cost effective and efficient, silicon is a highly durable material that can withstand harsh weather conditions and has a long lifespan. These factors make silicon a highly desirable material to use for solar cell production. Figure 2.1 is an example of what SoG-Si looks like before it is processed into a solar panel.

Figure 2.1: Pure silicon [21]

2.1.2 Production process

Pure silicon that is needed for solar panels cannot be found naturally and must be refined instead. As mentioned earlier, silicon can be found in great abundance and makes up for 28% of the mass found in earth's crust [5]. Usually, silicon is found in the form of quartz or other rocks and sands [7]. This quartz then undergoes silica extraction in order to extract the silicon dioxide (SiO_2). The SiO_2 that was obtained from the quartz sand is subjected to multiple different processing steps. By inducing a carbothermic reduction of SiO_2 in a submerged arc furnace, the first step is taken in producing what is known as metallurgical grade silicon (MG-Si). This metallurgical grade silicon has a purity between 96-98% silicon. Within the arc furnace, the reaction that is taking place can be seen in reaction (1).

$$SiO2 + 2C \rightarrow Si + 2CO \qquad (1)$$

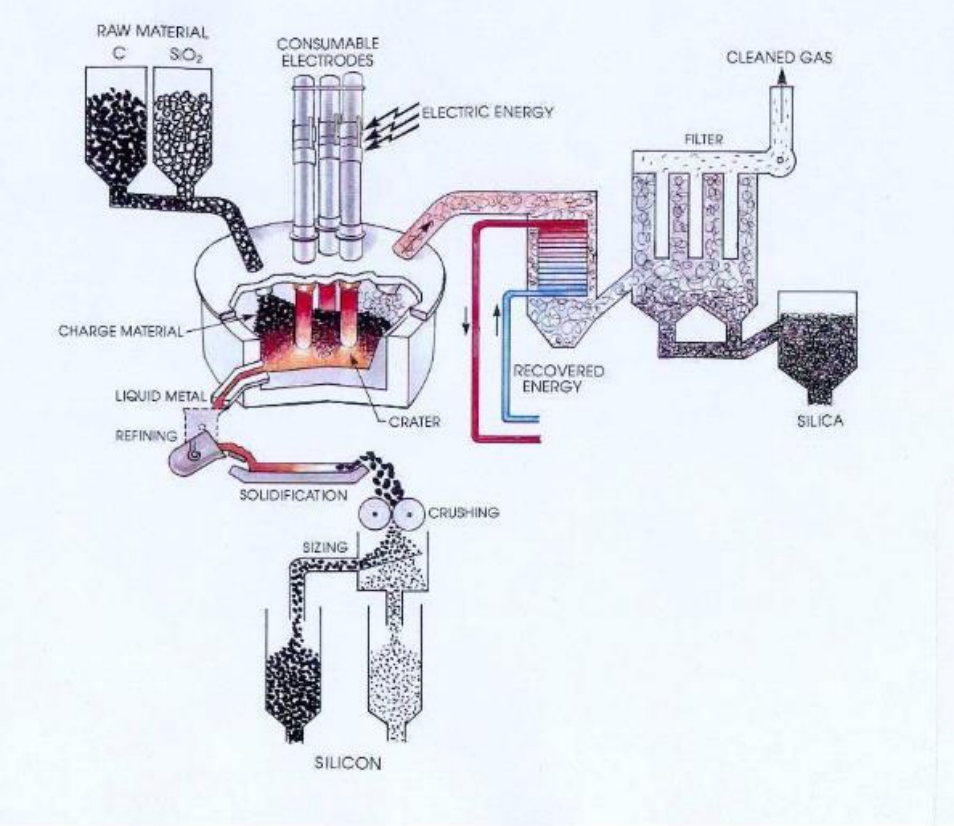

Figure 2.2: The process of using and submerged arch furnace to produce MG-Si **[**22**]** .

A submerged arc furnace is used because it can reach the necessary temperatures at which silicon gets reduced. Figure 2.2 depicts the entire process the SiO_2 undergoes before it becomes MG-Si. Along the top of the furnace, SiO_2 is added along with carbon (C), while the tapping of MG-Si can be seen towards the bottom of the arc furnace. Charge materials are loaded into the furnace where three electrodes are submerged into the charge to supply a three-phase current that passes through the furnace's contents. The current heats a portion of the charge to around 2000°C in the furnace's hottest area [8]. The process in which silicon becomes MG-Si is a complex process. The furnace can be divided into 3 different parts. The combustion zone, the low temperature zone, and the high temperature zone. The combustion zone is where the raw materials are charged and are exposed to oxygen. The following reactions take place in the combustion zone. The following reactions (2) and (3) take place in the combustion zone.

$$SiO(g) + 0.5O_2 = SiO_2(s,) \quad (2)$$

$$CO + 0.5\ O_2 = CO_2 \quad (3)$$

In the combustion zone silicon monoxide gas (SiO) and carbon monoxide gas (CO) gas from the charge will enter and react with oxygen from the air, resulting in oxidation as seen in reactions (2) and (3). As the SiO gas oxidizes it will begin to form SiO_2 particles. These particles are known as micro silica as seen in reaction (2). The solid SiO_2 and gaseous CO_2 produced during this process will exit the furnace. This by-product of SiO_2 is widely utilized across various industries, including construction, chemical, and oil and gas industries. As the charge materials descend into low temperature zone, the following 3 reactions start to take place as seen in reactions (4) to (6).

$$SiO(g) + 2C(s) = SiC(s) + CO(g) \quad (4)$$

$$3SiO(g) + CO(g) = SiC(s) + 2SiO_2(l) \quad (5)$$

$$2SiO(g) = Si(l) + SiO_2(l) \quad (6)$$

The low temperature zone's temperature can range anywhere between 700°C – 1300°C [9]. At this stage in the process, SiO_2 and C will interact with the SiO and CO gasses what were produced in the inner zone. Some of the SiO gas will react with carbon materials, resulting in the formation of

silicon carbide gas (SiC) as can be seen in reaction (4). The reaction is crucial since it captures SiO gas and produces SiC, which is the primary reactant for silicon formation reactions in the furnace's inner zone. When the temperature reaches a range of 1900°C -2000°C the materials arrive at the high temperature zone where reactions (7) to (9) take place.

$$2SiO_2(s,l) + SiC(s) = 3\,SiO(g) + CO(g) \quad (7)$$

$$SiC(s) + SiO(g) = 2\,Si(l) + CO(g) \quad (8)$$

$$SiO_2(s,l) + Si(l) = 2SiO(g) \quad (9)$$

SiC and SiO_2 undergo a reaction that results in the production of liquid silicon, SiO gas, and CO gas, as shown in reactions (7) to (9), After the liquid silicon has reached its extraction point within the furnace, it is released through a taphole found towards the bottom of the arc furnace. From there, it undergoes additional refinement processes such as slag treatment and gas purging. The impurities in the molten silicon are oxidized by purging it with oxygen (O), resulting in the formation of the slag layer. Impurities such as boron (B), aluminium (Al) and calcium (Ca) can easily be removed during this process [10]. After removing the layer of slag, the molten silicon is then allowed to cool in the desired mould and crushed to the desired size.

The production of silicon that is used in solar cells requires an extremely high purity, and for silicon to be graded as SoG-Si, it must have a purity of 99.9999%(6N). The MG-Si produced in the submerged arc furnace only has a purity of around 96-98% as noted earlier in section 2.1.2. Additional refining steps are required to achieve the necessary level of purity needed for solar panels. The two primary methods used to refine MG-Si to solar-grade silicon are the metallurgical method and the chemical method. In Norway the metallurgical method is the preferred method and REC solar uses a method known as the ELKEM Solar process [9]. The chemical method also known as the Siemens process, is more commonly used in other countries as the preferred commercial method.

The Siemens process comprises of three distinct stages. In the first stage begins with the gasification of MG-Si. At temperatures of around 300°C, the MG-Si is combined with hydrochloric acid (HCl). This process produces a gaseous mixture of silicon, hydrogen (H), and

chlorine (Cl) caused by the heating of HCl acid. The resulting gas is then cooled and condensed into a liquid, as seen in reaction (10).

$$5Si + 16HCl \rightarrow 4HSiCl_3 + 6H_2 + SiCl_4 \qquad (10)$$

The next stage of the Simens process involves distillation, which is used to eliminate impurities such as boron. Boron is an important impurity to remove during this stage as it negatively impacts the electrical qualities of SoG-Si. As the distillation phase nears its end and enters the next phase of silicon deposition, silane gas is produced [11]. The silane gas is then heated, resulting in the formation of solid silicon and hydrogen, as demonstrated reaction (11).

$$HsiCl_3 + H_2 \rightarrow Si + 3HCl \qquad (11)$$

The metallurgical process for SoG-Si production from primary raw materials is the ELKEM Solar process and it can be divided into three phases as well. The first step of the refining process involves slag treatment, in which raw MG-Si is melted along with slag to extract boron from the silicon. This is accomplished by melting the MG-Si with calcium silicate slag (CaO-SiO2), as seen in reaction (12).

$$4B + 3\,SiO_2 \rightarrow 2B_2O_3 + 3Si \qquad (12)$$

After removing the slag and allowing the substance to cool and solidify, the material may need to be crushed and prepared for leaching. This entails treating the crushed material with an acidic solution like HCl. The silicon crystals are then leached in the acid solution, and once the leaching process is complete, the crushed silicon crystals are then remelted and solidified into larger pieces. The solidification stage is the final stage of the process. As the silicon cools and solidifies, the impurities will remain in their liquid form, allowing it to be easily removed [10].

2.1.3 Leaching background information

In metallurgy, leaching is a hydrometallurgical method that is used to extract valuable metals from ores and other solid materials by dissolving them in a liquid solvent or solution that is used as an extraction medium. If a material is leached in a way that the impurities are dissolved and removed, it is a leaching-refining process. The material that is leached is typically crushed and then mixed with a suitable solvent such as water or a chemical solution such as HCl. These impurities can then be washed, filtered, and processed in order to give pure metal. There are many different types of solvents that can be used for leaching such as, sulfuric acid (H_2O_4) and ammonium hydroxide (NH_4OH) and there are also many different types of leaching methods that can be utilized such as in-situ leaching, heap leaching and pressure leaching [12]. These different types of leaching processes offer flexibility and adaptability for extracting valuable substances from solid materials in various industries, including mining, metallurgy, and environmental remediation. The choice of leaching method depends on factors such as the characteristics of the material being leached, the desired outcome, economic considerations, and environmental considerations.

The leaching method can be used to refine the silicon-kerf used in experimental work using acid leaching, as this study. Acid leaching is a cost-effective and commonly used method used to purify MG-Si [13]. It offers flexibility in treating MG-Si and defending on what purity of silicon is needed, acid leaching can either be used to treat the silicon before it undergoes the main refinement process, or it can be used as the main method of silicon refinement. The effectiveness of acid leaching relies on the segregation behaviour of impurities during the solidification process of molten silicon. Along the grain boundaries of MG-Si, impurities will precipitate during the solidification of molten silicon [14]. When the MG-Si is then crushed and introduced to acid leaching, most of the impurities will then be exposed amongst the surface of the silicon. These impurities can then be easily removed by leaching using solvents or acidic solutions. Acid leaching is useful for removing impurities due to their high segregation behaviour, however, impurities such as boron and phosphorus have large segregation coefficients. By alloying with reactive metals such as calcium, the leaching extraction of phosphorus can be significantly improved. This additional step helps address the limitations and enhance the efficiency of the acid leaching process [13].

2.1.4 Melting of silicon

There are various additives that can be added to silicon before the melting process. In the experimental work, FBR Si (Fluidized bed reaction silicon) and $CaO\text{-}SiO_2$ slag is added to the kerf in the melting process. $CaO\text{-}SiO_2$ is a slag that is often added alongside silicon during the production process of MG-Si or SoG-Si via the Elkem process. $CaO\text{-}SiO_2$ can participate in slag formation when combined with silicon in a furnace. Slag is a material that forms during the smelting or refining of metals. It helps to separate impurities from the desired metal and provides a protective layer over the metal surface, preventing oxidation or contamination. FBR Si is a silicon that has undergone a fluidized bed reactor process. The FBR process uses seed granules that are continuously fed into a chamber with heated silane gas entering from below and exiting above. The circulation of gas causes the seed granules to flow like a liquid as the silane gas breaks down and deposits silicon layers on the granules as the hydrogen is removed and recycled. Over time, the granules grow larger, heavier, and eventually tapped from the bottom of the chamber. According to REC silicon, the FBR method results in an 80-90% reduction in energy consumption. The reason that FBR Si is mixed along with the silicon kerf is to aid in the melting process since the silicon kerf powder is difficult to melt [15].

When silicon oxidizes in a furnace during melting, it undergoes a chemical reaction with oxygen in the atmosphere, resulting in the formation of SiO_2, commonly known as silica. The oxidation of silicon can occur when molten silicon comes into contact with oxygen or other oxidizing agents present in the furnace environment. The melting point of SiO_2 is higher than the melting point of silicon. As oxidation occurs, the presence of silica can raise the melting point of the mixture and ruin the sample as it heats in the furnace. There are two methods that can be used to prevent oxidation during the melting process. By either using an induction furnace that has a vacuum chamber that removes the oxygen, or by utilizing inert gas to create an inert atmosphere which protects the samples from oxidation. Argon is a noble gas, which means it is chemically inert. It does not readily react with other elements or compounds under normal conditions [16]. This inertness makes argon an ideal choice for creating an environment that minimizes unwanted chemical reactions or oxidation. Argon is also a monatomic gas, consisting of individual atoms. It lacks reactive components like oxygen, moisture, or other reactive gases that can initiate or participate in chemical reactions. By purging or replacing the atmosphere with argon, these

reactive components are effectively removed, reducing the likelihood of unwanted reactions and oxidation.

2.1.5 Silicon kerf

When silicon ingots are cut and wafered, a portion of the material is lost, which is known as silicon kerf. The cutting and wafering process for solar silicon accounts for 19% of the total production costs [17], and up to 50% of the silicon is lost due to mixing with the sawing liquid or debris [3]. Before silicon ingots can be cut and wafered, they must be squared up by cutting and grinding the edges and ends to create a perfect rectangular shape with clean, straight edges and corners. This process removes about 10% of the ingot and helps eliminate any surface irregularities or impurities, making it easier to handle and process the ingot further [18].

Once the silicon ingot has been squared up and prepared, it can be cut into silicon wafers. Two common methods for cutting silicon ingots are the diamond saw and the multiwire saw. The multiwire saw method has two variations: the loose abrasive method and the fixed abrasive method. Figure 2.3 depicts how a multiwire cuts the silicon ingot in order to produce silicon wafers. When using a multiwire saw, the entire ingot is cut at once using a wire with a diameter of 80-120µm [17] and the resulting wafer thickness is between 100-200µm. The loose abrasive technique utilizes a mixture of polyethylene glycol and abrasive silicon carbide particles in the form of a slurry, which is applied to the ingot alongside the wire. The cutting action is achieved by the friction generated by the slurry. In contrast, the fixed abrasive approach employs diamond particles directly affixed to the wire. As the wire traverses the ingot, these abrasive particles cut through the silicon.

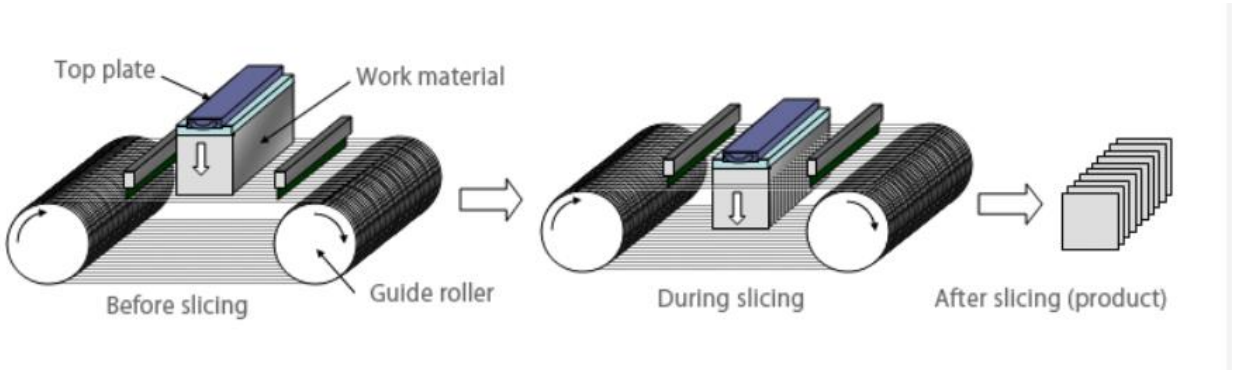

Figure 2.3: Schematic of multiwire sawing of Si ingot for wafer production **[**19**]**.

2.1.6 Silicon kerf recycling

The thickness of the saw blade used in the cutting process determines the amount of kerf lost. Thicker blades typically result in larger amounts of kerf loss, but they also result in less breakage and more uniformity in the wafer thickness. Thinner blades can result in less kerf loss, but they are more likely to break the wafers and result in more variation in the wafer thickness. After the entire cutting and wafering process is finished, approximately 50% of the silicon ingot is lost during the entire process. Although no recent studies have shown the amount of waste produced, approximately 101,750 tons of waste were produced in 2010 [18]. Since the industry has grown substantially since then, it is reasonable to assume that waste production has also increased since 2010. The problem with silicon kerf is that it is extremely difficult and time-consuming to separate the high purity silicon from the SiC particles. Many companies ignore and throw away any SiC particles that are smaller than 5um. Regardless of the difficulty, there are still many methods that are used to recycle and reuse silicon kerf. Filtration, sedimentation, directional solidification, and centrifugal separation are just a few of the recycling methods that can be used to separate the silicon kerf from its impurities [3].

2.1.7 Solar cells

There are 3 types of silicon solar cells that are being produced today in the photovoltaic industry and the percentage of annual production can be seen in Figure 2.4. Monocrystalline solar cells are the first type of solar cells used today and they are made from a single crystal of silicon and have a uniform, flat black appearance. They are the most efficient type of solar cell, with an efficiency rate of up to 22%, but they are also the most expensive, having a production rate of around 12%. Polycrystalline solar cells are the second type, and they are made by melting multiple fragments of silicon together. They have a blue colour and a speckled appearance due to their irregular crystal structure. They are less expensive than monocrystalline cells, but they are also less efficient, with an efficiency rate of around 15% while having a production rate of around 82%.

The third and final type of solar cell used today is a Thin-film solar cell. These solar cells are made by depositing a thin layer of semiconductor material, such as silicon or cadmium telluride, onto a substrate. They are much less expensive to produce than monocrystalline or polycrystalline cells, but they are also less efficient, with an efficiency rate of around 10% and with a production rate of around 6%. However, thin-film cells can be made flexible and lightweight, making them useful for certain applications such as building-integrated photovoltaics [19] [20].

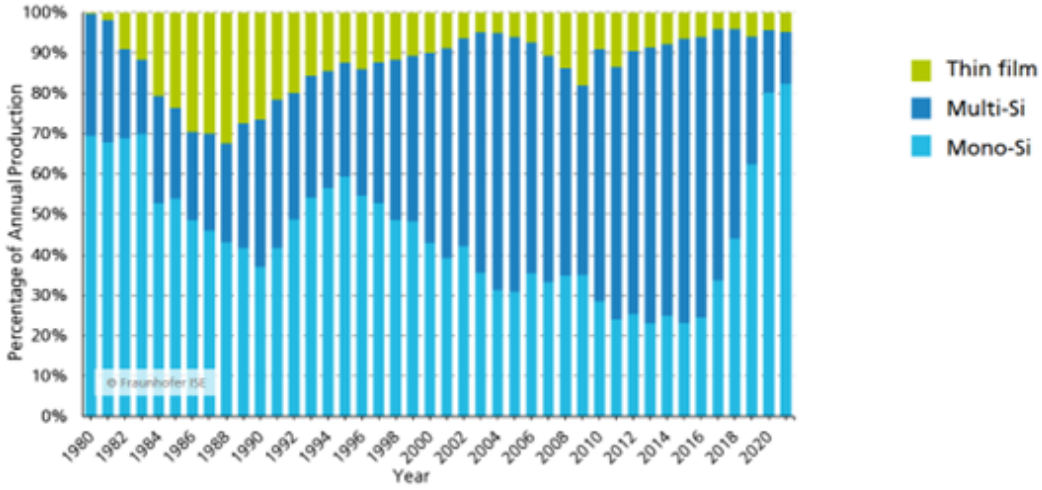

Figure 2.4: Production numbers for the 3 types of solar cells **[21]**.

3. Experimental procedure

The following figures 3.1 and 3.2 show the experimental plan and data parameters that were used in the experimental procedure.

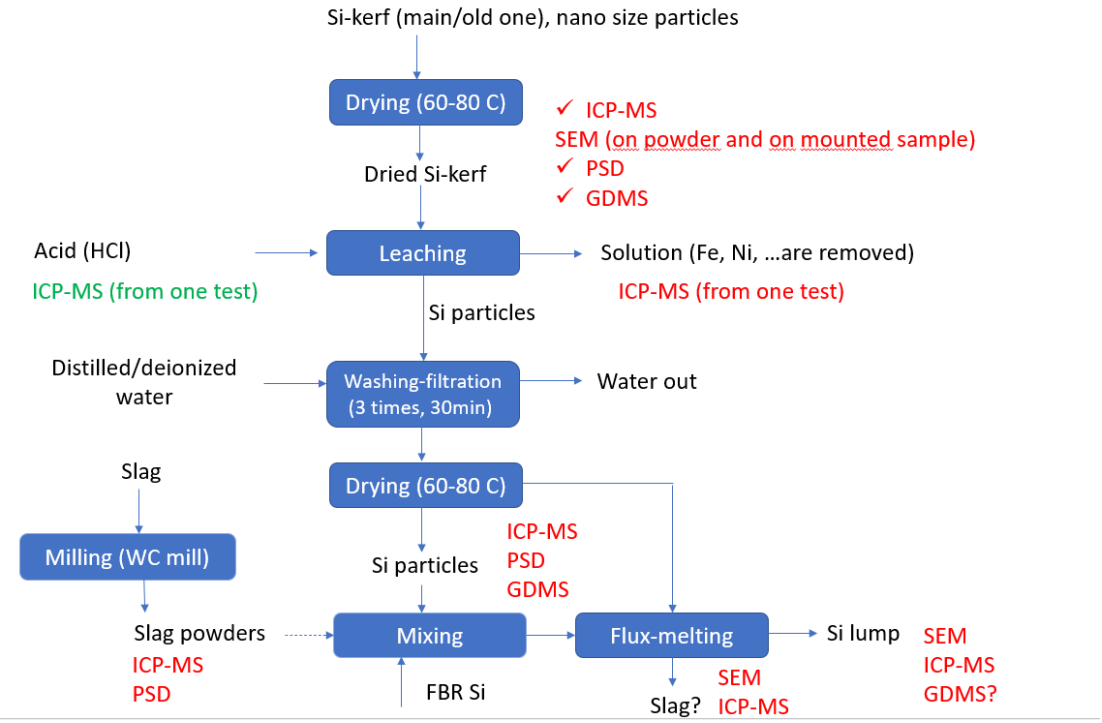

Figure 3.1: The experimental plan that was used to carry out the experimental procedures.

Exp nr.	Slag type or FBR Si	Wt% Slag	Slag/FBR mass (g)	Temperature	Duration	Comment
1	-	0	0	1650	60 min	Pressed sample
2	-	0	0	1650	120 min	Cut crucible
3	CaO-SiO2	2	2	1650	60 min	Cut crucible
4	CaO-SiO2	5	5	1650	60 min	Cut crucible
5	CaO-SiO2	10	10	1650	60 min	Cut crucible
6	CaO-SiO2	20	20	1650	60 min	Cut crucible
7	FBR Si	-	2	1600	60 min	Cut crucible
8	FBR Si	-	5	1600	60 min	Cut crucible
9	FBR Si	-	10	1600	60 min	Cut crucible
10	FBR Si	-	20	1600	60 min	Cut crucible

Figure 3.2: The data parameters used during the melting process of the experimental procedure.

3.1 Material preparation and leaching

Before the leaching process can begin, the kerf needs to be treated in a drying oven for at least 24 hours at temperatures of 60°C-80°C to remove as much moisture as possible. Silicon, when exposed to moisture, the kerf can react with oxygen in the air and undergo oxidation, resulting in the formation of SiO_2 or other oxidized compounds. By drying the silicon kerf, moisture is either eliminated or significantly reduced. As a result, the chances of silicon coming into contact with moisture is minimized. A total of 1kg needs to be dried for the amount of kerf needed, however, due to material loss in the leaching and the washing process, more should be prepared just in case. The dried kerf was then crushed using a mortar and pestle. The kerf powder was then ready to be leached. A sample of dried kerf before it was crushed and leached can be seen in Figure 3.3.

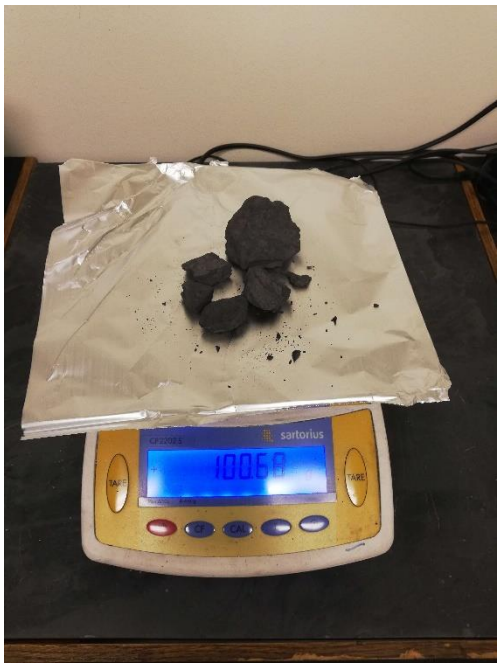

Figure 3.3: A sample of dried silicon kerf

The kerf powder was then poured into a beaker along with a 1M HCl acid solution. For every 100g of kerf powder, 1 litre of 1M HCl acid solution was used. A magnetic field created by a magnetic mixer was placed within the beaker to promote mixing. The beaker was then placed upon a hotplate and leached at a temperature of 40°C for a duration of 60 minutes with a stirring rate of 300RPM

(revolutions per minute). Once this step was completed, the beaker was taken off the hotplate and prepared for the next step in the process which is filtering. Figure 3.4 shows 2 samples of silicon kerf being leached.

Figure 3.4: 2 samples of kerf undergoing leaching.

The liquid kerf mixture was then poured into 4, 5cm x 9cm containers which were then placed inside the VWR Megastar 600 centrifuge as seen in Figure 3.5. The centrifuge was then turned on for 15 minutes at 4000RPM. This allows the centrifuge to separate the mixture and leave behind a concentrated silicon sludge. This process was repeated until the entire liquid silicon mixture had been filtered and all that remained was the concentrated silicon sludge. This sludge was then placed into a beaker again and mixed with 1 litre distilled water and was placed upon the hotplate to undergo further washing.

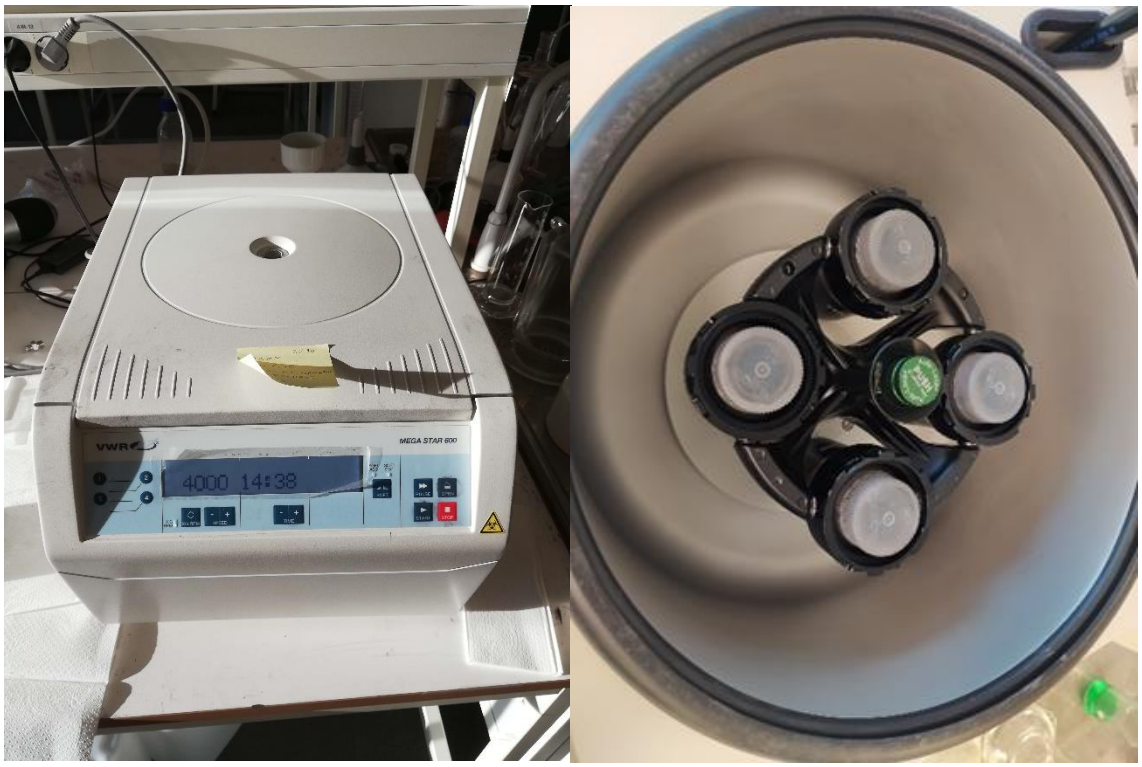

Figure 3.5: The VWR Megastar 600 centrifuge used to separate the silicon kerf sludge.

The same parameters used for the leaching process are used for the washing process but instead of a duration of 60 minutes, it was washed for duration of 30 minutes. Once the mixture was finished washing, it was once again filtered and separated by using the centrifuge. This washing/filtering process was repeated 3 times to properly wash and filter the kerf. Once the kerf had been properly washed and filtered, the remaining silicon kerf sludge was then placed in a beaker and was once again put back in the drying oven at a temperature between 60°C-80°C for 2-4 days to properly dry and remove the moisture from the kerf sludge. Once the kerf was properly dried, it was ready for the next stage of the process which was treating the dried kerf in an induction furnace. Figure 3.6 shows what the silicon kerf looks like after the entire leaching and drying process is completed.

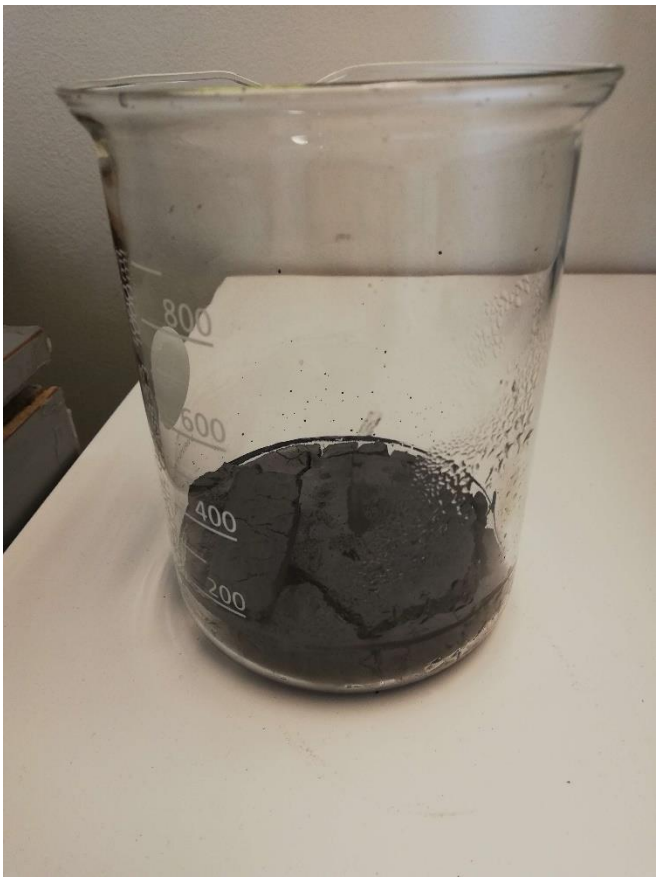

Figure 3.6: A sample of dried kerf that has undergone the entire leaching process.

3.2 Melting of leached Si-kerf

The IF75 induction furnace was used for the melting process of the silicon kerf. Depending on the experiment, the samples mixtures were prepared slightly differently. For all experiments the dried kerf was crushed into a fine power and mixed with the additives before being pressed into 3 smaller 5cm x 18cm graphite crucibles. The 3 crucibles were then placed inside a larger 15cm x 32cm graphite crucible. For experiments 1-2 only the kerf powder was added to the crucibles as experiments 1-2 were conducted without any additives. For experiments 3-6 the silicon kerf was crushed and mixed alongside the $CaO\text{-}SiO_2$ slag powder before being poured and pressed into the crucibles. For experiments 7-12 the silicon kerf powder was mixed with the FBR Si granules before being poured and pressed into the crucible. Each crucible was then weighed before and after the experiment in order to properly record the loss in mass. The smaller crucibles were then covered

with a graphite lid to limit oxidation and were then put inside the larger crucible. The larger crucible was then placed inside the induction furnace and was covered with a graphite lid. All 3 small crucibles placed within the larger crucible can be seen in Figure 3.7.

Figure 3.7: 3 samples are placed in smaller crucibles which were then placed in a larger crucible before beginning the melting process.

The graphite lid has 3 holes but only 2 are utilized for the melting process. The first hole holds the alumina insulating tube containing the thermocouple which is used to measure the temperature of the furnace. The second hole is used to insert the gas tube which releases the argon gas used to create the inert atmosphere which helps limit the silicon oxidation. Since there was no use for the third hole on the lid, it was covered with a piece of graphite to further prevent oxidation. Once the crucible was fully prepared, the induction furnace was turned on along with the ventilation tube. As the furnace is heated to the desired temperature, 1650°C for experiments 1-6 and 1600°C for experiments 7-12, the ventilation tube absorbs any gases released during the melting process. Once the furnace had reached the desired temperature, it was left to melt and heat the samples for the set amount of time. After the desired duration, the furnace was turned off and left to cool until the crucible could be handled. Once the crucibles were fully cooled, they could be taken out, weighed, and moved on to the next stage of the refinement process. Figure 3.8 shows the induction furnace turned on and heating a sample of silicon kerf.

Figure 3.8: The IF75 induction furnace used to melt the silicon kerf. A points towards the thermocouple, B points towards the argon gas tube, C points towards the covered lid hole, D points towards the ventilation tube, E points towards the main graphite crucible and F points towards the furnace body.

3.3 Characterization of samples

The crucibles containing the melted silicon kerf, were then filled with an epoxy mixture, and left untouched again until the epoxy mixture was completely dry. It is important to have the sample embedded in epoxy as it helps to stabilize and allows for a flat and planar finish during the polishing. Once it was dry the crucible was then cut in half using a diamond saw. A diamond saw must be used as other sawblades are not capable of cutting through solid silicon. Once the crucible had been cut and the sample had been prepared to the desired size, it was ready to move on to the next stage which was polishing.

Figure 3.9: The Struers LaboPol-21 that was used for polishing along with the 2 different types of test samples that were polished.

The sample then goes through 5 polishing stages using a Struers LaboPol-21 which can be seen in Figure 3.9. The first step in the polishing process is to remove the scratches that were caused by cutting the crucible. By using a Molto 220 grinding disc and turning on the water flow, the sample was firmly pressed upon the disc and polished. Then the sample was polished on a new grinding disc, a Piano 600, where it was further polished along with water. Once the sample had been polished sufficiently, it was then polished using a Lagran 9 grinding disc along with a 15um diamond suspension used to assist in the polishing of the sample. The abrasive nature of diamond particles allows for precise and controlled material removal, resulting in a smooth and reflective surface finish. Once the sample had been polished using the diamond suspension, it was cleaned using an ultrasonic cleaner and isopropanol for 2 minutes. Once that sample had been cleaned, it was dried using compressed air to quickly remove all the moisture. The sample was then polished using an Allegran 3 grinding disc along with a 3um diamond suspension. Once it had been polished

sufficiently, it was once again cleaned in the ultrasonic cleaner for 5 minutes. Then the sample was polished using a Chemal polishing disc along with an OP-U suspension used for final finishes. The sample was then put in a vacuum chamber for a minimum of 3 hours so that enough moisture was removed. These steps must be repeated for every single sample before they can be analysed further.

3.3.1 Scanning electron microscopy (SEM)

A Hitachi S-3400N scanning electron microscope (SEM) was used for high-resolution imaging and analysis of sample's surfaces. SEM provides detailed 3D images of the samples by scanning a focused electron beam across their surfaces and detecting various signals generated in response to the interaction between the beam and the sample. Before images of the samples can be taken, they need to be prepared by adding a coating to increase the conductivity [22]. SEM imagery requires a conductive surface to prevent the build-up of static charges that can distort the image and affect the electron beam. Materials like carbon or gold are usually used for this, however aluminium foil can also be wrapped around the sample to provide an increase in conductivity. Pictures are then taken at different magnifications in order to get high resolution images of the sample's surface. After the desired images were taken, the SEM was used to map the elements using energy dispersive x-ray spectrometry (EDS) found on the sample. EDS was used to analyse specific points on the image to get accurate elemental details. EDS was also used to analyse certain areas of the image and map out all the different elements found on the sample. This process must be repeated for all 12 samples. The schematics and working principles of a SEM microscope can be seen in Figure 3.10.

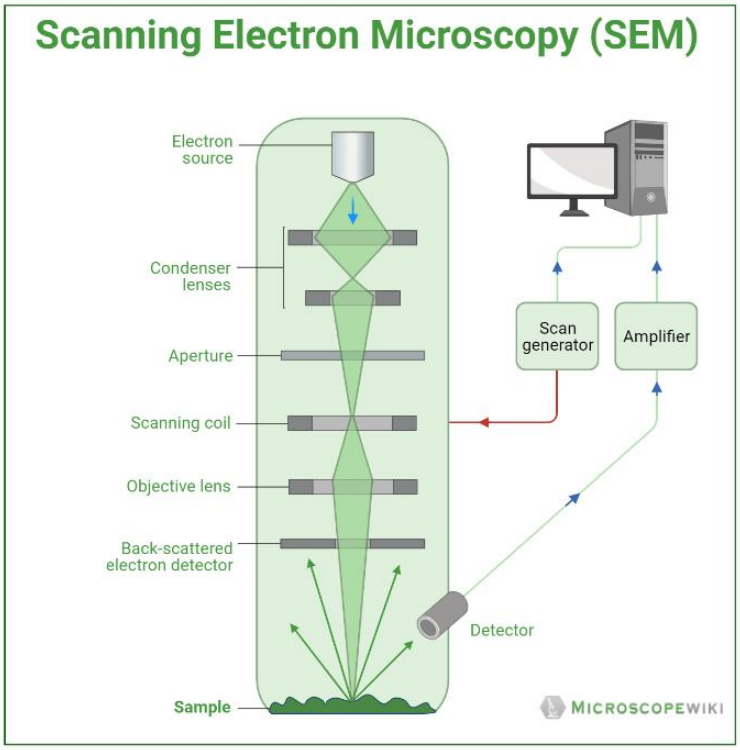

Figure 3.10: Schematics of a SEM microscope [22].

3.3.2 Glow discharge mass spectrometry (GD-MS)

An Astrum Glow discharge mass spectrometry (GD-MS) was used as an analytical technique to determine the elemental composition and isotopic ratios of the test samples [23]. It combines the principles of glow discharge spectroscopy (GDS) and mass spectrometry (MS) to provide information about the elemental composition and concentration of a material. In this case GD-MS was used to analyse a sample of silicon kerf before it had been leached, a sample of silicon kerf after it was leached and a sample of silicon kerf that underwent the entire refining process. The schematics and working principles for GD-MS can be seen in Figure 3.11.

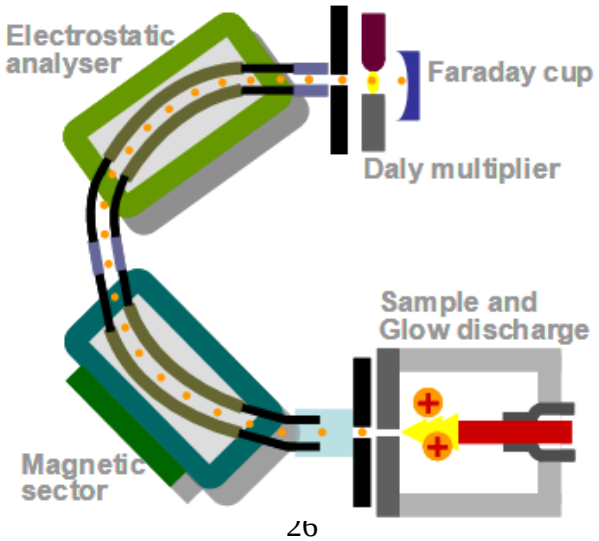

Figure 3.11: Schematic of GD-MS [26].

3.3.3 Inductively coupled plasma mass spectrometry (ICP-MS)

Inductively coupled plasma mass spectrometry (ICP-MS) is an analytical technique used for the determination of trace and ultra-trace elements in a variety of samples. ICP-MS combines the principles of inductively coupled plasma (ICP) and mass spectrometry (MS) to achieve sensitive and accurate elemental analysis. Liquid samples are first introduced and broken down into their constituent elements. These elements are then transformed into ions using an ionization source, which generates an extremely high temperature of around 8000 °C. The resulting ions are subsequently directed into a mass spectrometer for measurement. ICP-MS offers exceptional sensitivity, allowing for the simultaneous determination of up to 70 elements in a single sample analysis [24]. All samples that were analysed via ICP-MS were sent to the ICP-MS laboratory at NTNU to be processed. Figure 3.12 shows the schematics and working principles for ICP-MS.

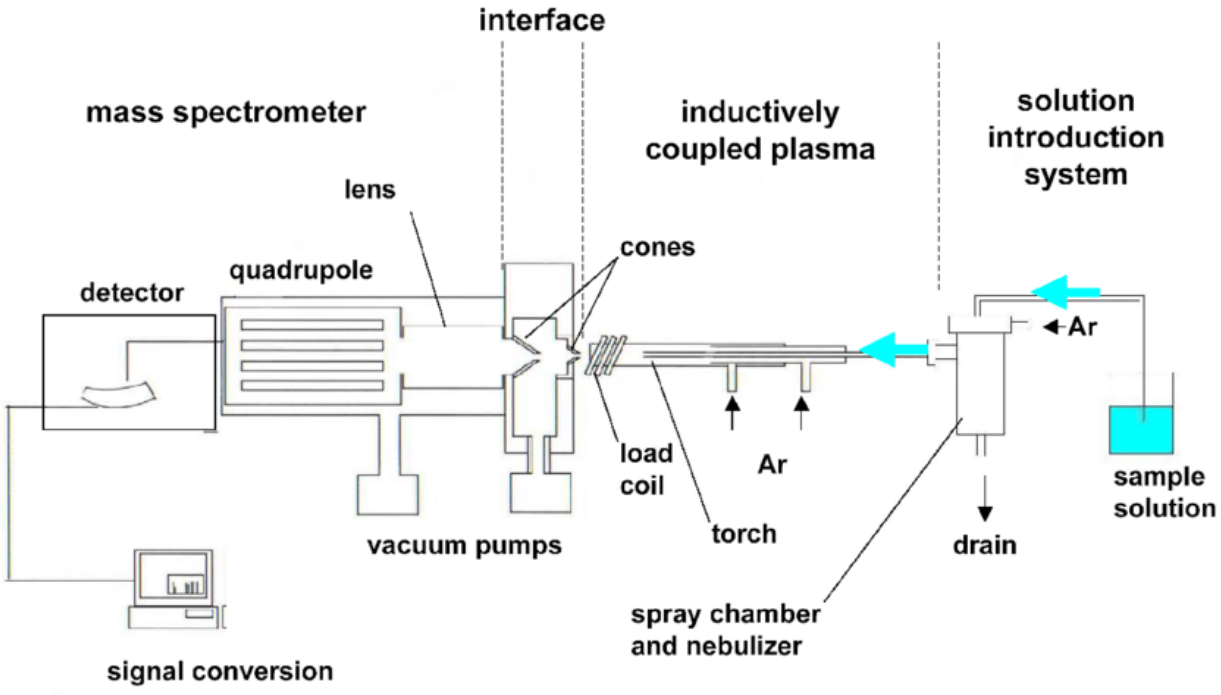

Figure 3.12: Schematics of ICP-MS [28].

4. Results

4.1 Analysis of silicon kerf and leached kerf

Figures 4.1 to 4.4 show the two different samples of silicon kerf, one sample that was analysed with a SEM microscope before it was leached and a sample of silicon kerf that was analysed after leaching. The SEM images were taken at different magnifications in order to better view the topography of the samples. EDS analysis was used to find which impurities were present in the samples before and after leaching. Tables 4.1 to 4.3 show two different samples of silicon kerf that were analysed by both ICP-MS and GD-MS, one sample before leaching and one sample after leaching. Both the ICP-MS and GD-MS analysis were used to see how much of the impurities were dissolved during the leaching and how much of those impurities remained after the leaching.

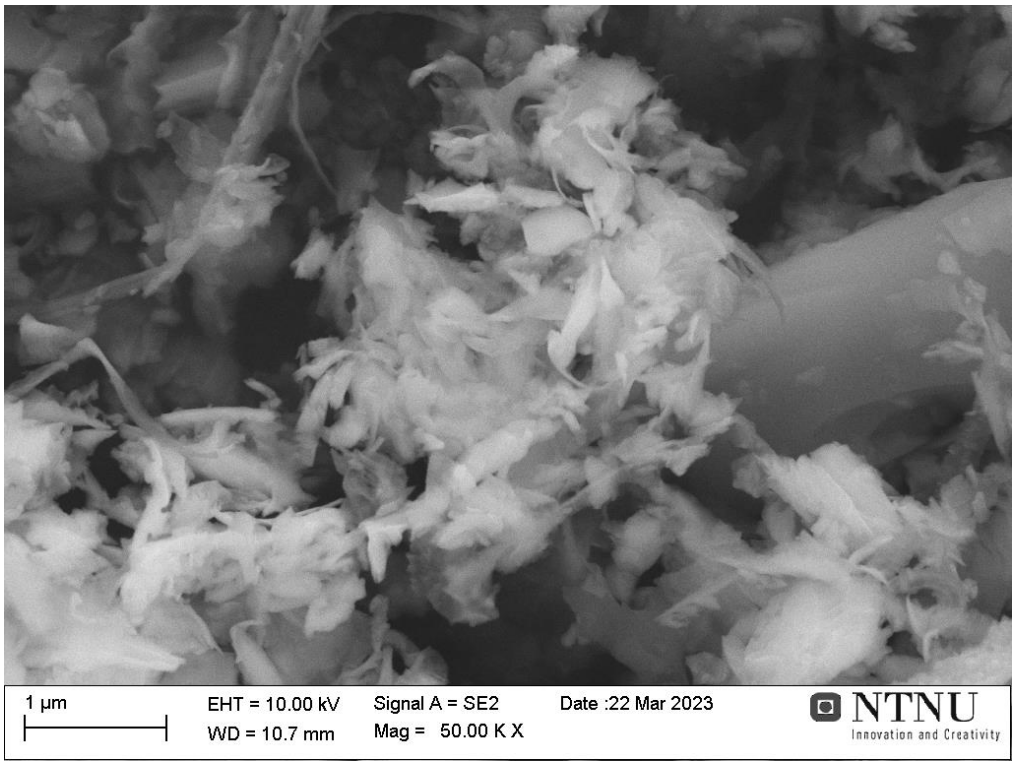

Figure 4.1: SEM imagery of a silicon kerf sample before it has undergone leaching.

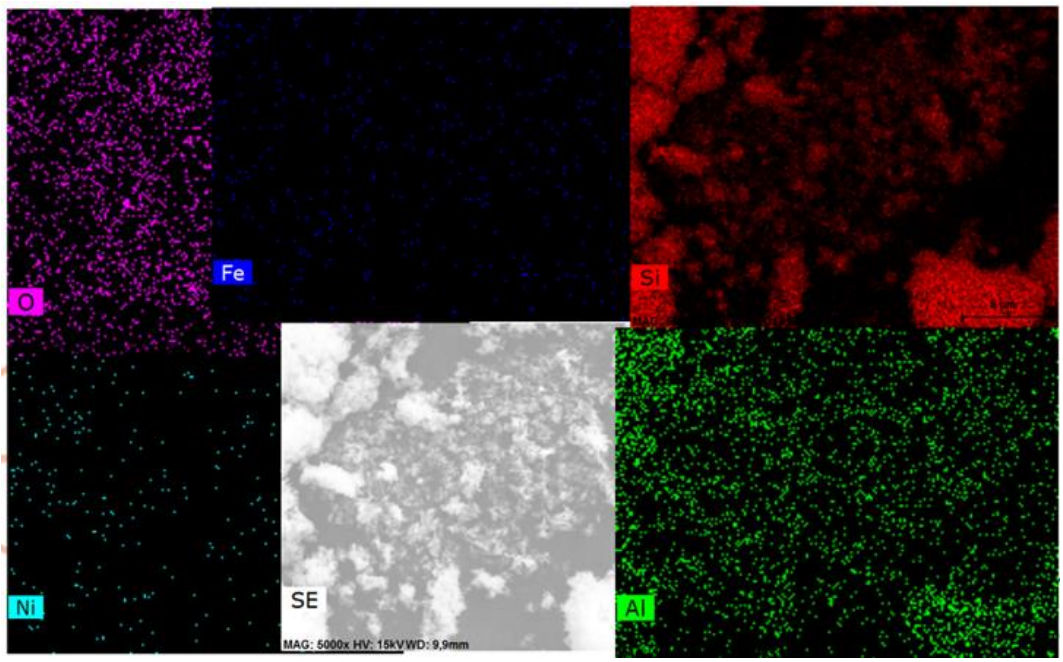

Figure 4.2: EDS elemental mapping showing the different trace elements found within the same silicon kerf sample from 4.1.

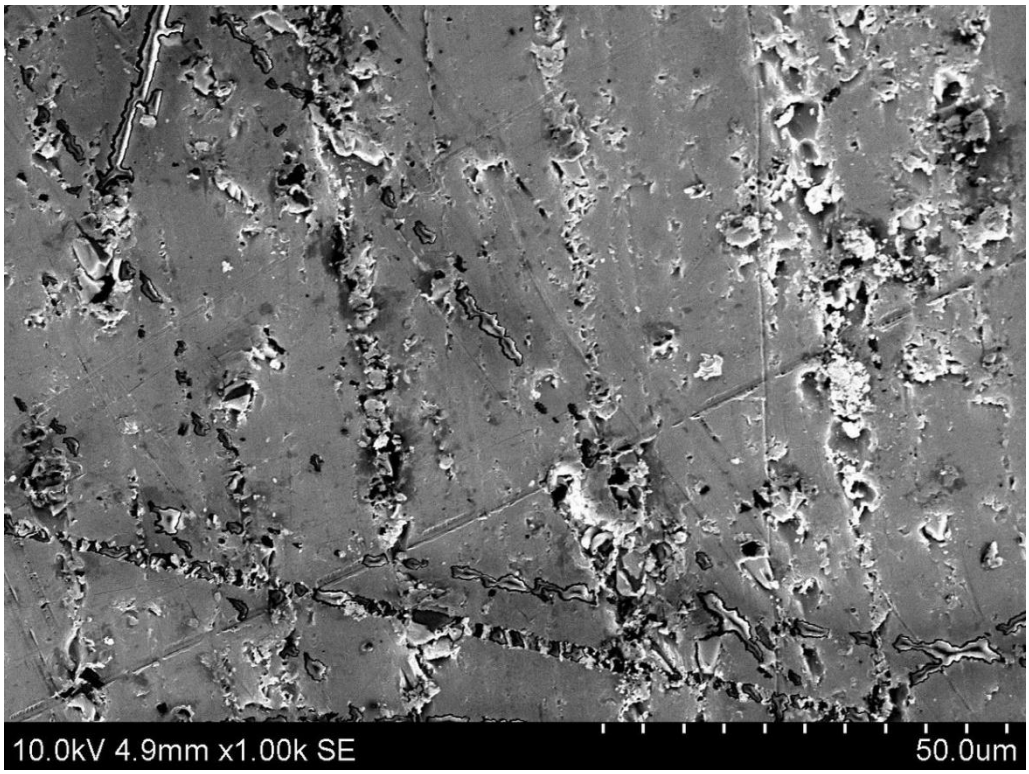

Figure 4.3: SEM imagery of a silicon kerf sample after the leaching process, the sample was mounted in an epoxy resin.

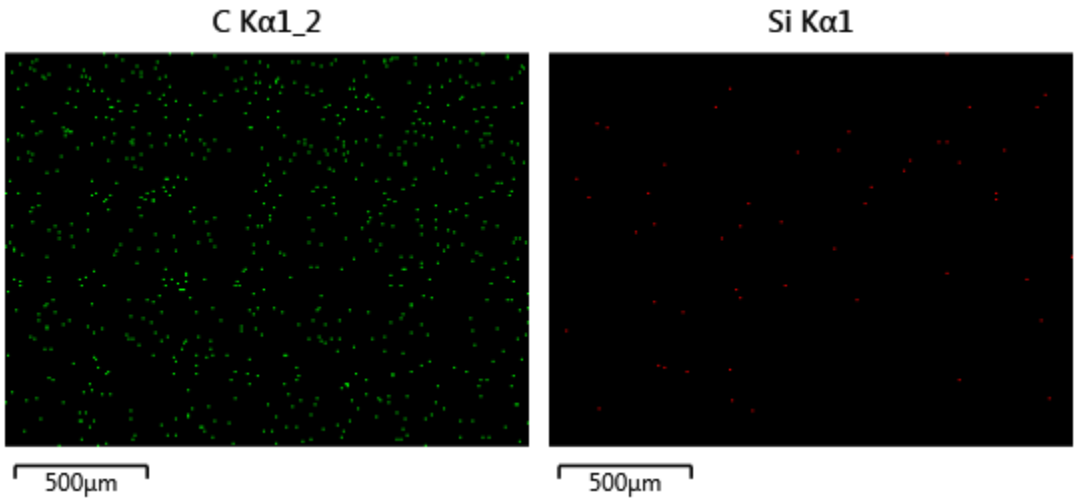

Figure 4.4: EDS elemental mapping showing the different trace elements found within the same silicon kerf sample from 4.3.

Table 4.1: ICP-MS results for the silicon kerf before leaching.

Element	**ppmw (parts per million by weight)**
Aluminium	9800
Boron	0.25
Calcium	14.6
Chromium	<0.7
Copper	0.7
Iron	2.5
Gallium	2.6
Magnesium	2.7
Manganese	<0.4
Nickel	113.9
Phosphorus	1.02
Titanium	3.4
Vanadium	<0.4

Table 4.2: GD-MS results for the silicon kerf before leaching.

Element	ppmw (parts per million by weight)
Aluminium	1100
Boron	0.44
Calcium	37.9
Chromium	0.49
Copper	2.1
Iron	195.9
Gallium	5.2
Magnesium	5.0
Manganese	2.5
Nickel	169.6
Phosphorus	9.8
Titanium	5.6
Vanadium	0.13

Table 4.3: GD-MS results for the silicon kerf after leaching.

Element	ppmw (parts per million by weight)
Aluminium	6800
Boron	2.02
Calcium	32.5
Chromium	1.2
Copper	3.1
Iron	33.2
Gallium	1.2
Magnesium	6.1
Manganese	1.7
Nickel	41.1
Phosphorus	2.6
Titanium	3.3
Vanadium	0.21

4.2 Furnace results

Figure 4.5 shows the temperature curve at which the furnace experiments were conducted. A stable temperature was held once the furnace reached the desired temperature for each experiment. In total 5 furnace experiments were conducted with 3 samples at a time, except for the last experiment, which was experiment 1, which was only conducted with 1 sample since experiment 1 was the only sample that would be in the furnace for 2 hours. Table 4.4 shows the parameters at which the experiments were conducted. The duration of the experiments, the amount of kerf, the number of additives to the kerf and the weight of the samples before and after the experiment can be seen. Obviously, there has been some weight loss in all experiments and the melting of Si-kerf is accompanied with some material loss at elevated temperatures.

Figure 4.5: A graph showing the temperature curves of the furnace experiments. The x axis is plotting the time in seconds while the y axis is plotting the temperature in Celsius.

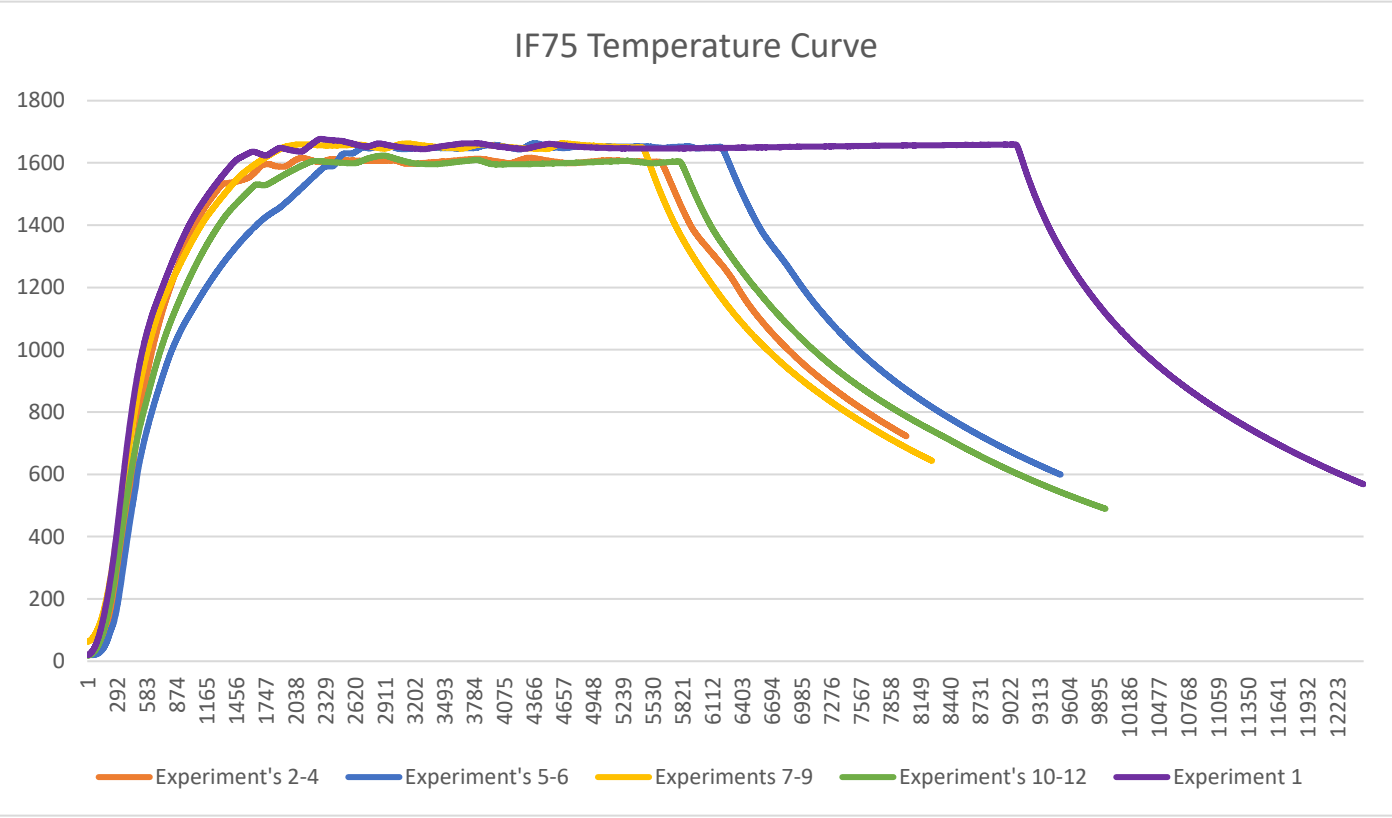

Table 4.4: The data parameters that were used for the furnace experiments as well as the before and after weight of the samples.

Experiments	Duration (minutes)	Wt% additives	Kerf mass (grams)	Additive mass (grams)	Initial weight (grams)	Weight loss (grams)
Experiment 1: No slag	120	0	100	0	310	269
Experiment 2: No slag	60	0	100	0	310	268
Experiment 3: CaO-SiO_2	60	2	98	2	310	264
Experiment 4: CaO-SiO_2	60	5	95	5	310	261
Experiment 5: CaO-SiO_2	60	10	57	5.7	273	252
Experiment 6: CaO-SiO_2	60	20	57	11.4	280	263
Experiment 7: FBR Si	60	2	98	2	310	280
Experiment 8: FBR Si	60	5	95	5	310	297
Experiment 9: FBR Si	60	10	90	10	310	285
Experiment 10: FBR Si	60	20	80	20	310	281
Experiment 11: FBR Si	60	30	70	30	310	288
Experiment 12: FBR Si	60	40	60	40	310	288

4.3 SEM results for melted samples

Figures 4.6 to 4.17 show the different SEM images taken for all 12 samples, which were prepared from the cut crucibles mounted in resin. The grey Figures are magnified by x65 and show the topography of the surface of the samples. Different spectrum points have been marked to indicate different phases within the sample. The elemental composition of these phases can be seen in table 4.5. The Figures that are in colour show the results from the EDS elemental mapping. These Figures show us which elements are found on the surface of the samples. Further SEM imagery taken with varying magnification and Figures showing the composition of each spectrum point measured in cps/eV can be found in the appendix.

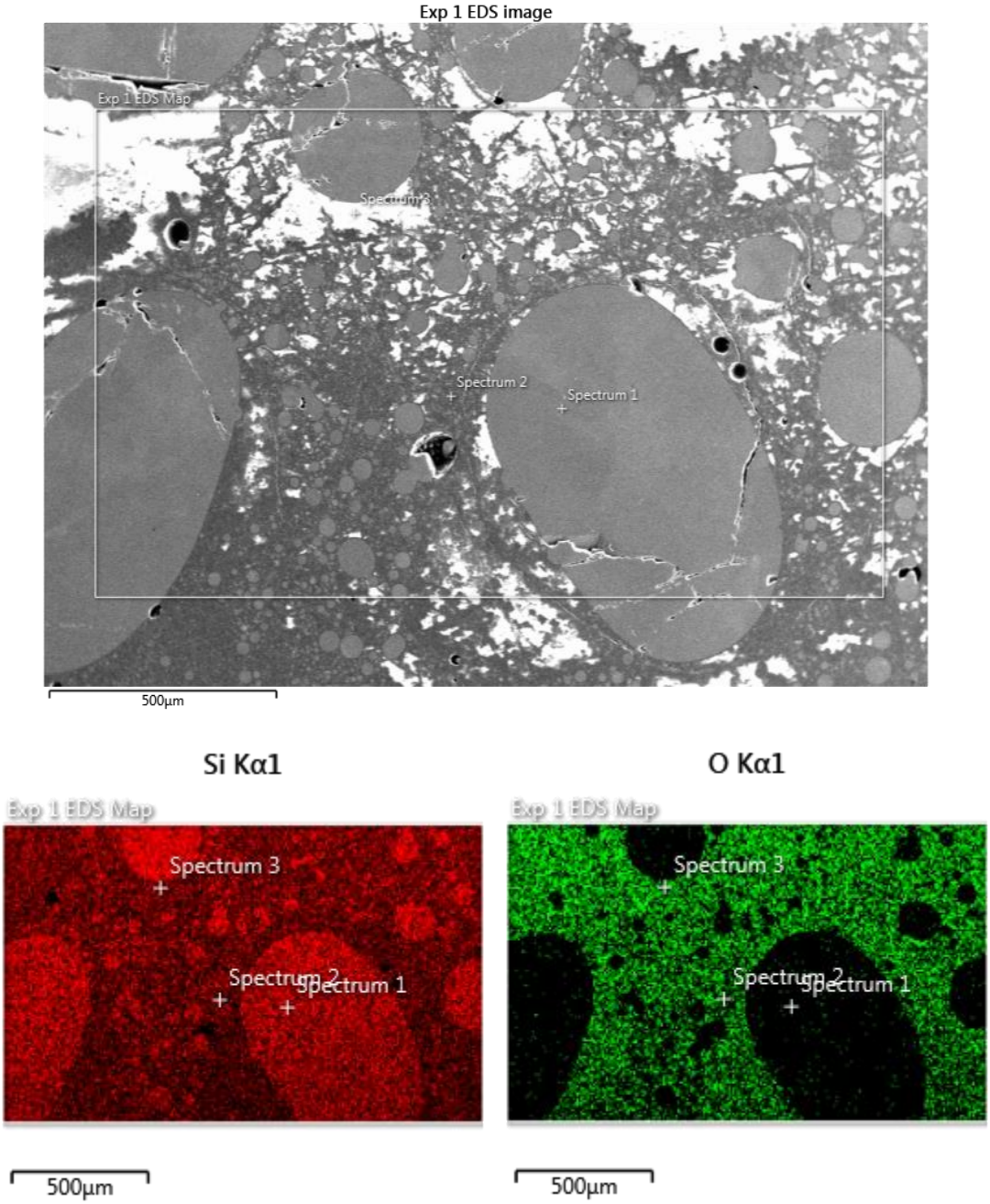

Figure 4.6: SEM and elemental X-ray mapping of experiment 1, taken at x65 magnification.

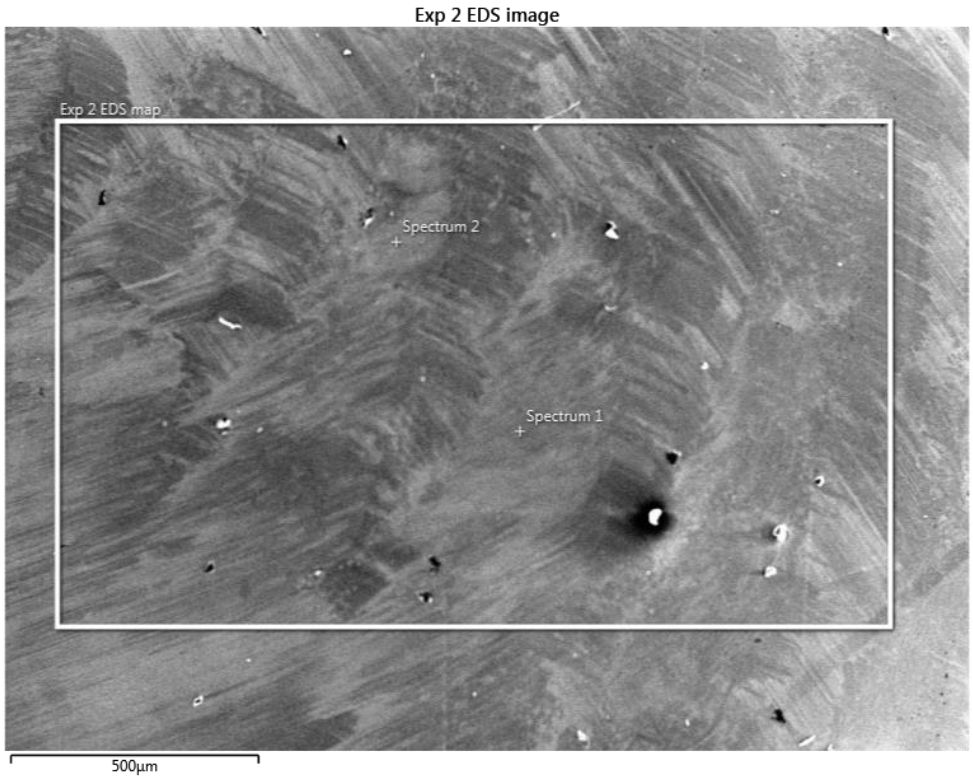

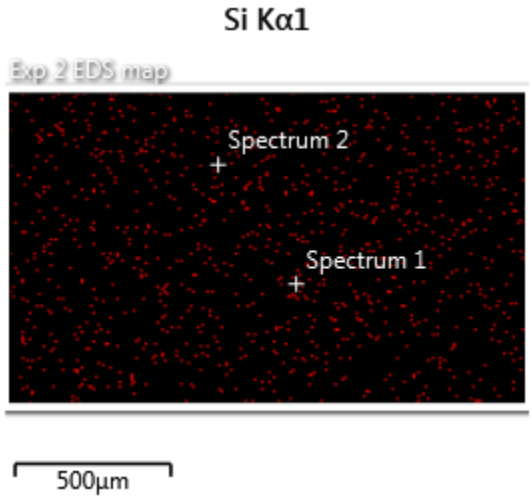

Figure 4.7: SEM and elemental X-ray mapping of experiment 2, taken at x65 magnification.

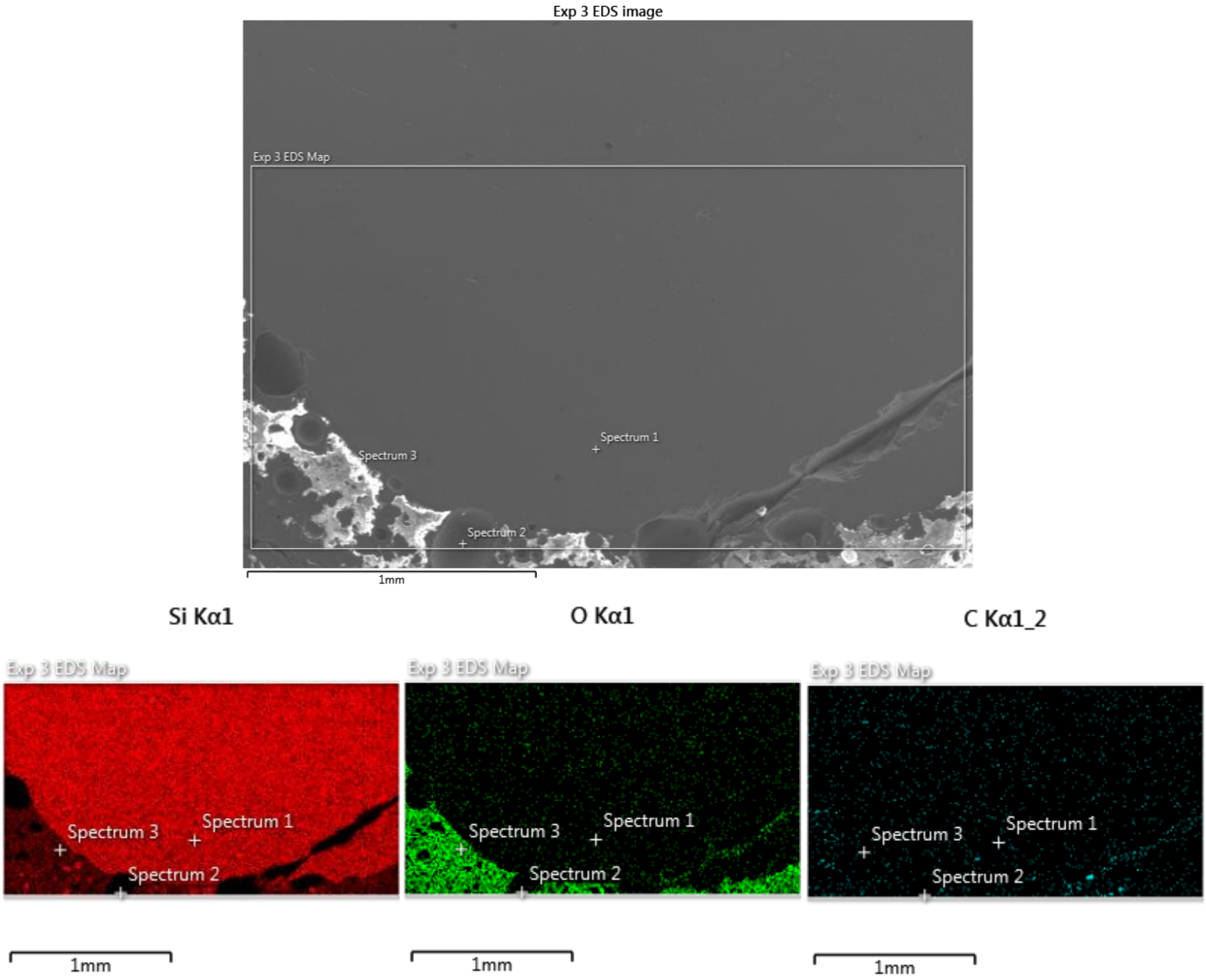

Figure 4.8: SEM and elemental X-ray mapping of experiment 3, taken at x65 magnification.

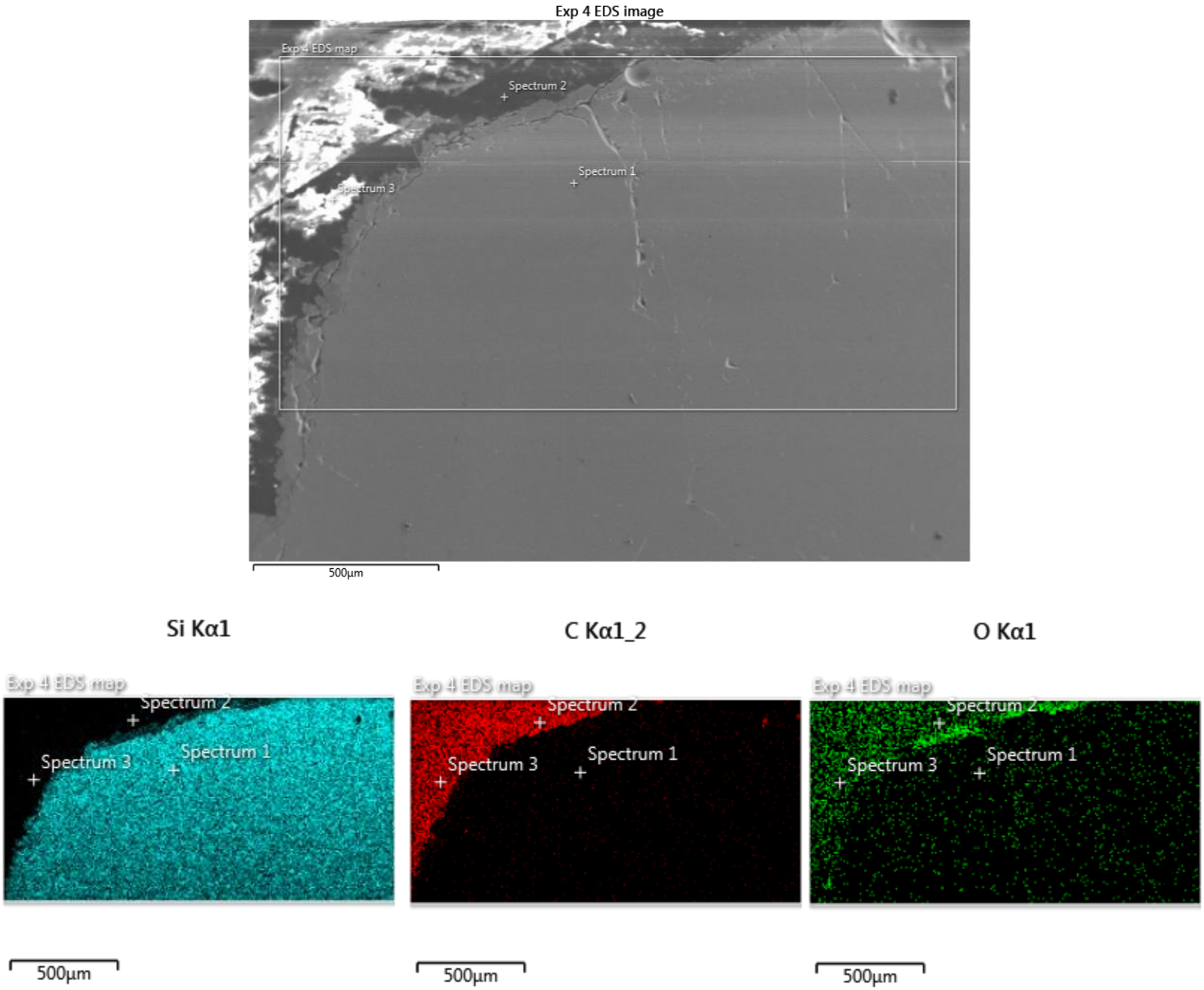

Figure 4.9: SEM and elemental X-ray mapping of experiment 4, taken at x65 magnification.

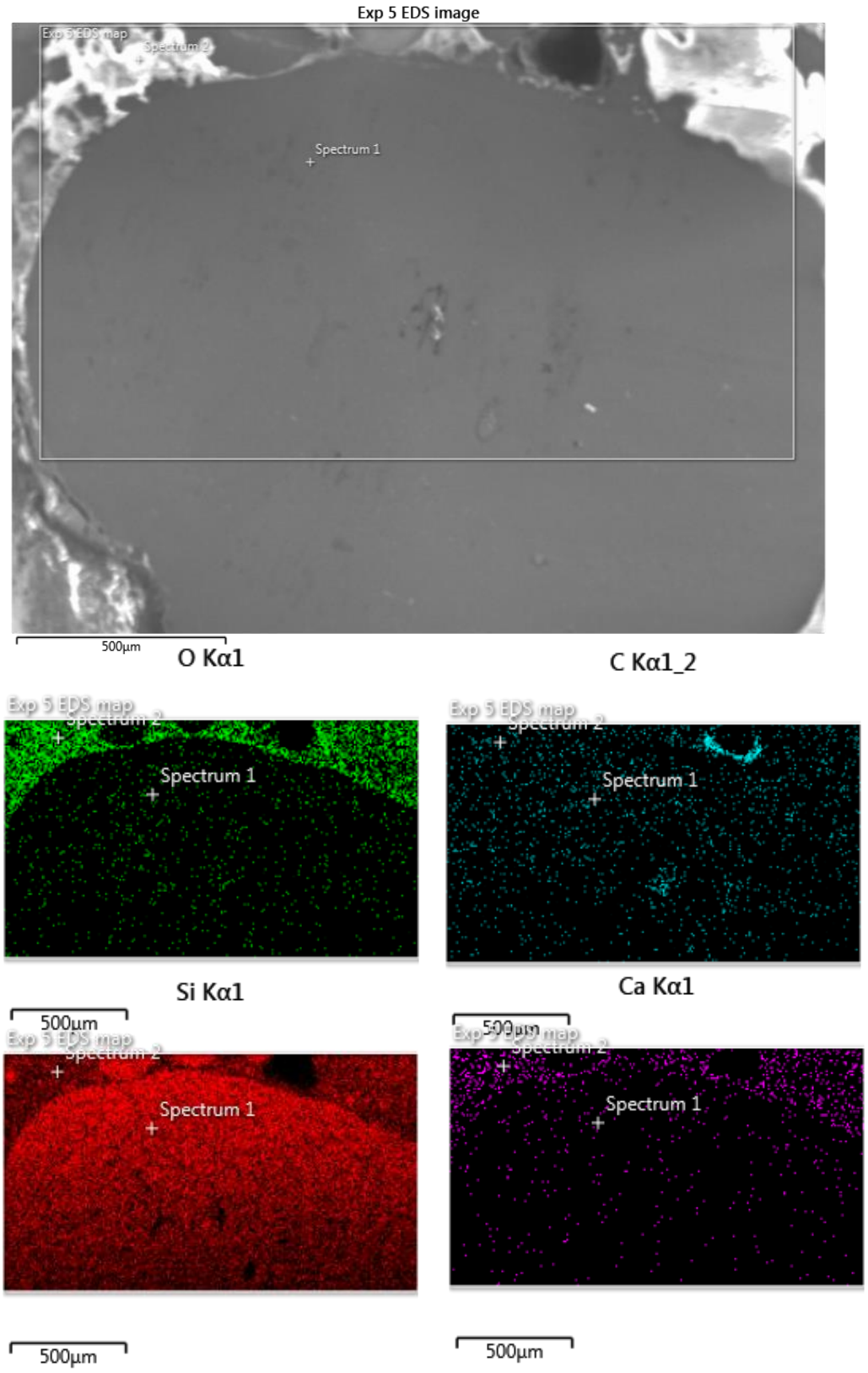

Figure 4.10: SEM and elemental X-ray mapping of experiment 5, taken at x65 magnification.

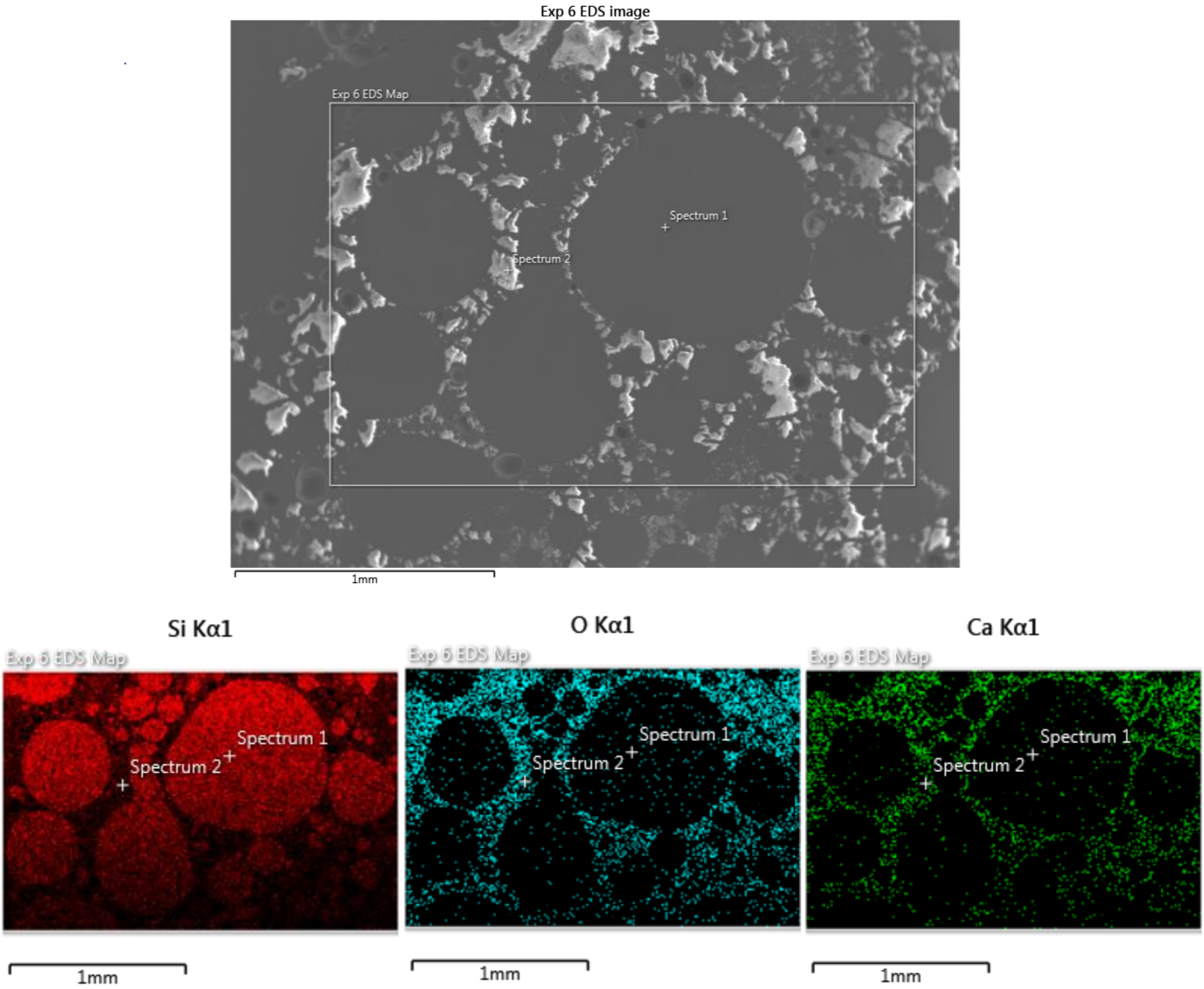

Figure 4.11: SEM and elemental X-ray mapping of experiment 6, taken at x65 magnification.

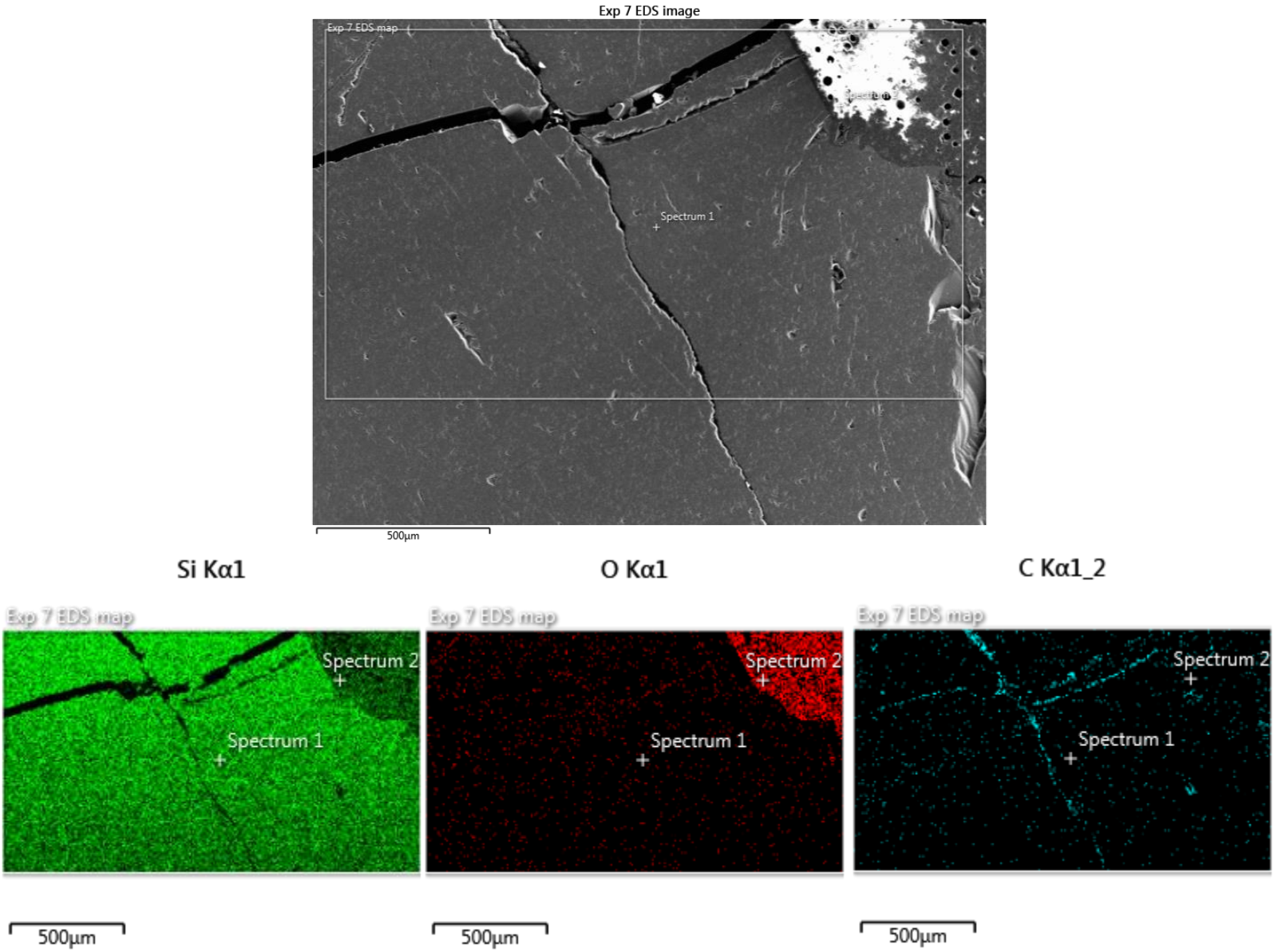

Figure 4.12: SEM and elemental X-ray mapping of experiment 7, taken at x65 magnification.

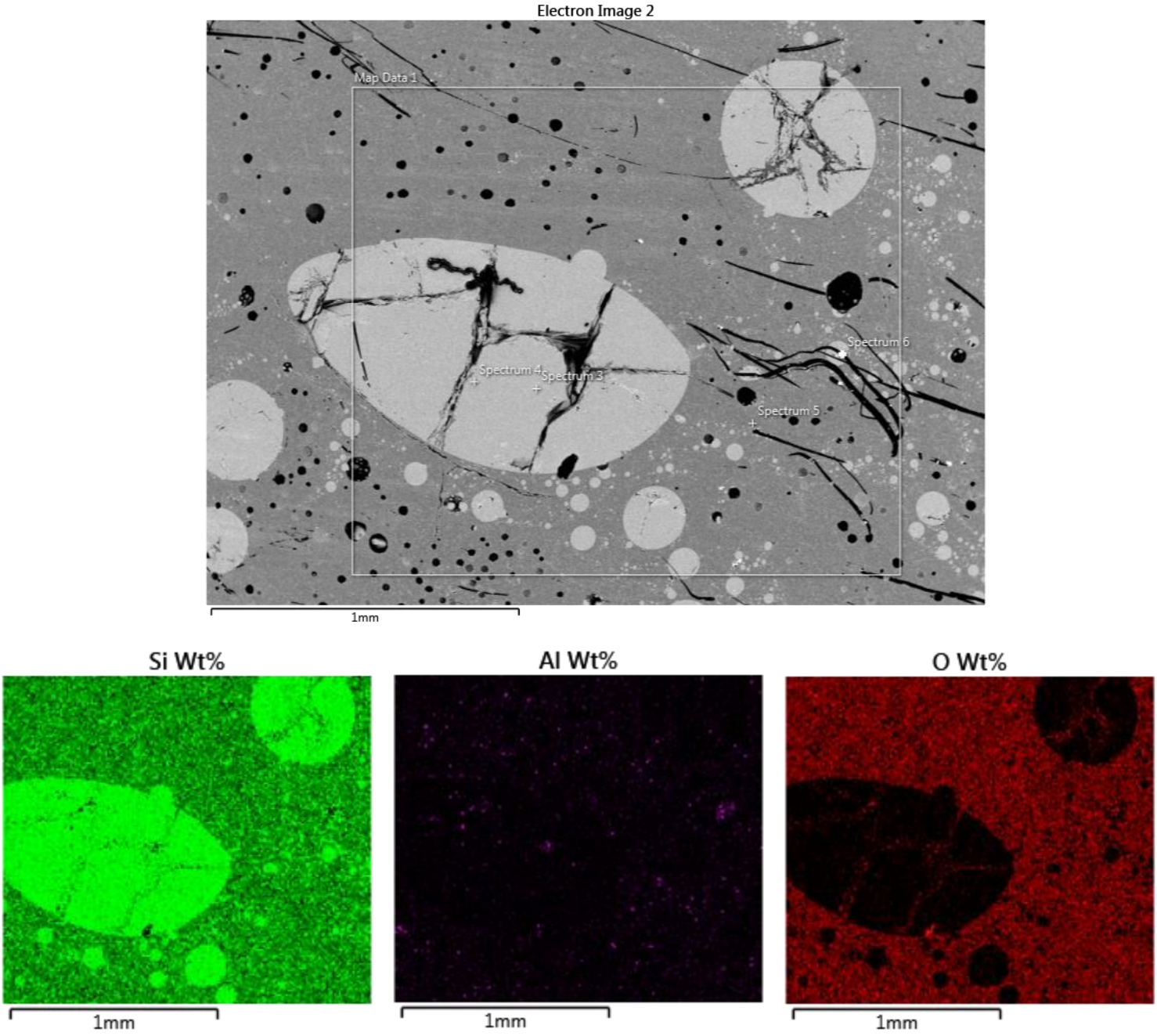

Figure 4.13: SEM and elemental X-ray mapping of experiment 8, taken at x65 magnification.

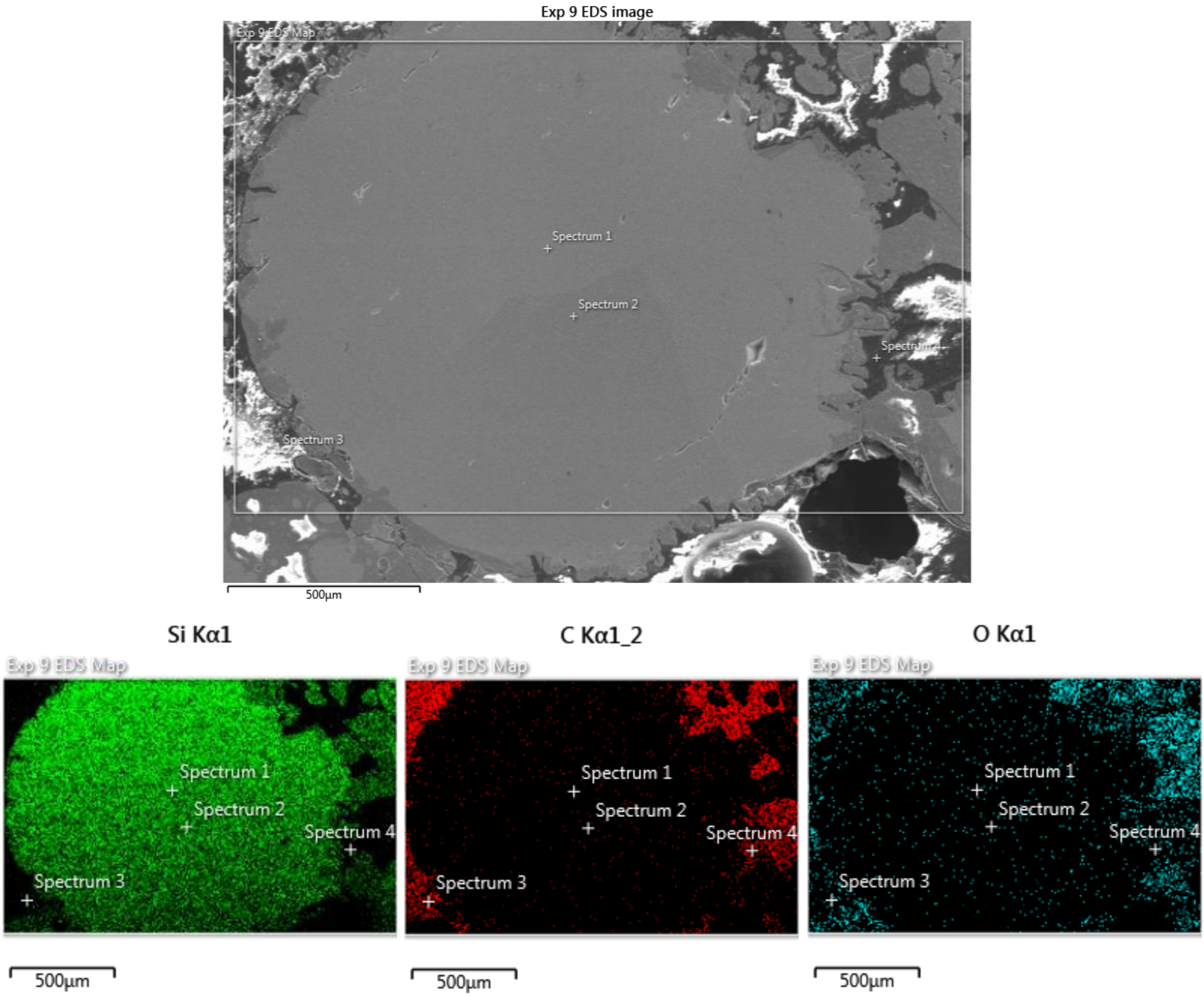

Figure 4.14: SEM and elemental X-ray mapping of experiment 9, taken at x65 magnification.

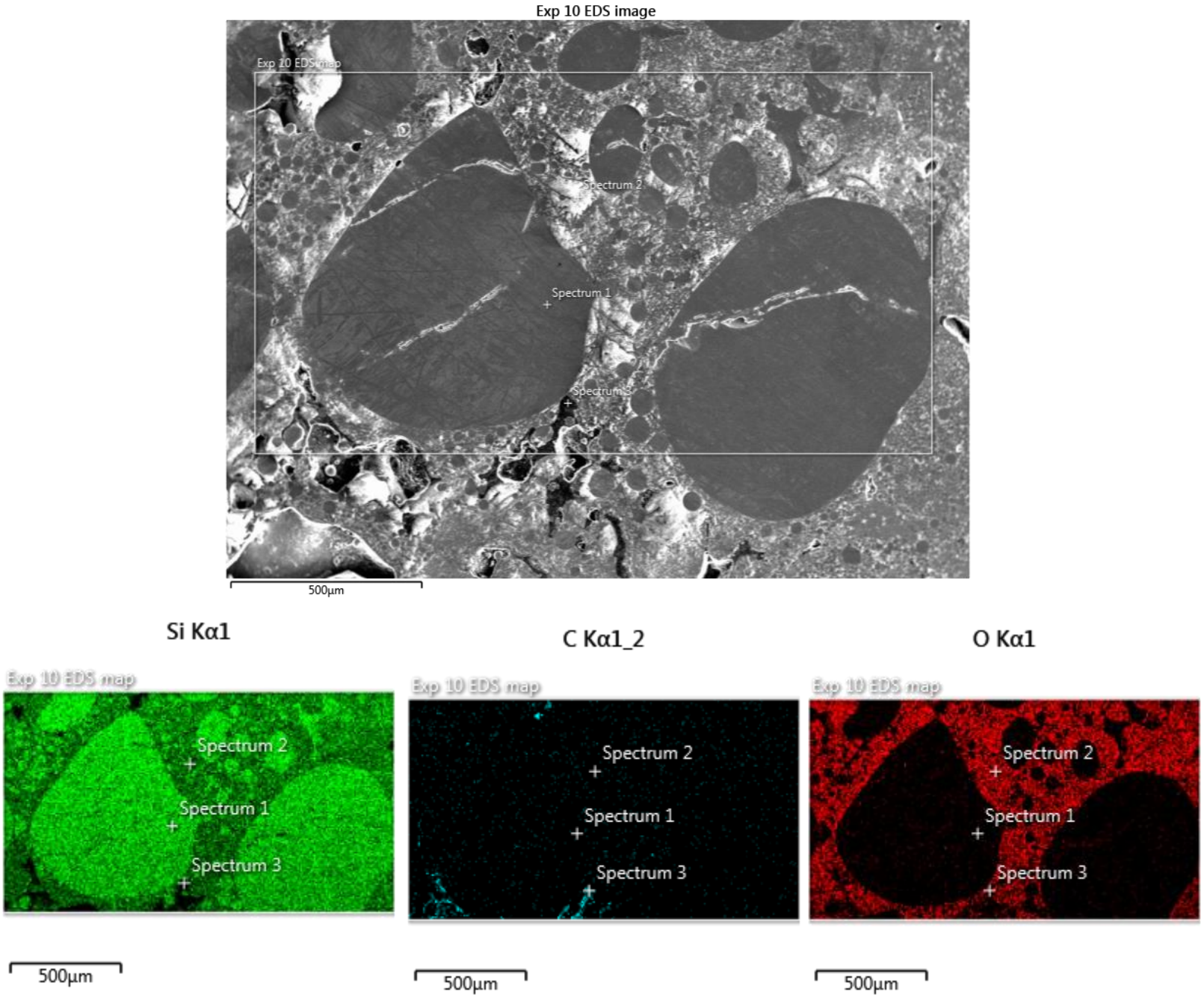

Figure 4.15: SEM and elemental X-ray mapping of experiment 10, taken at x65 magnification.

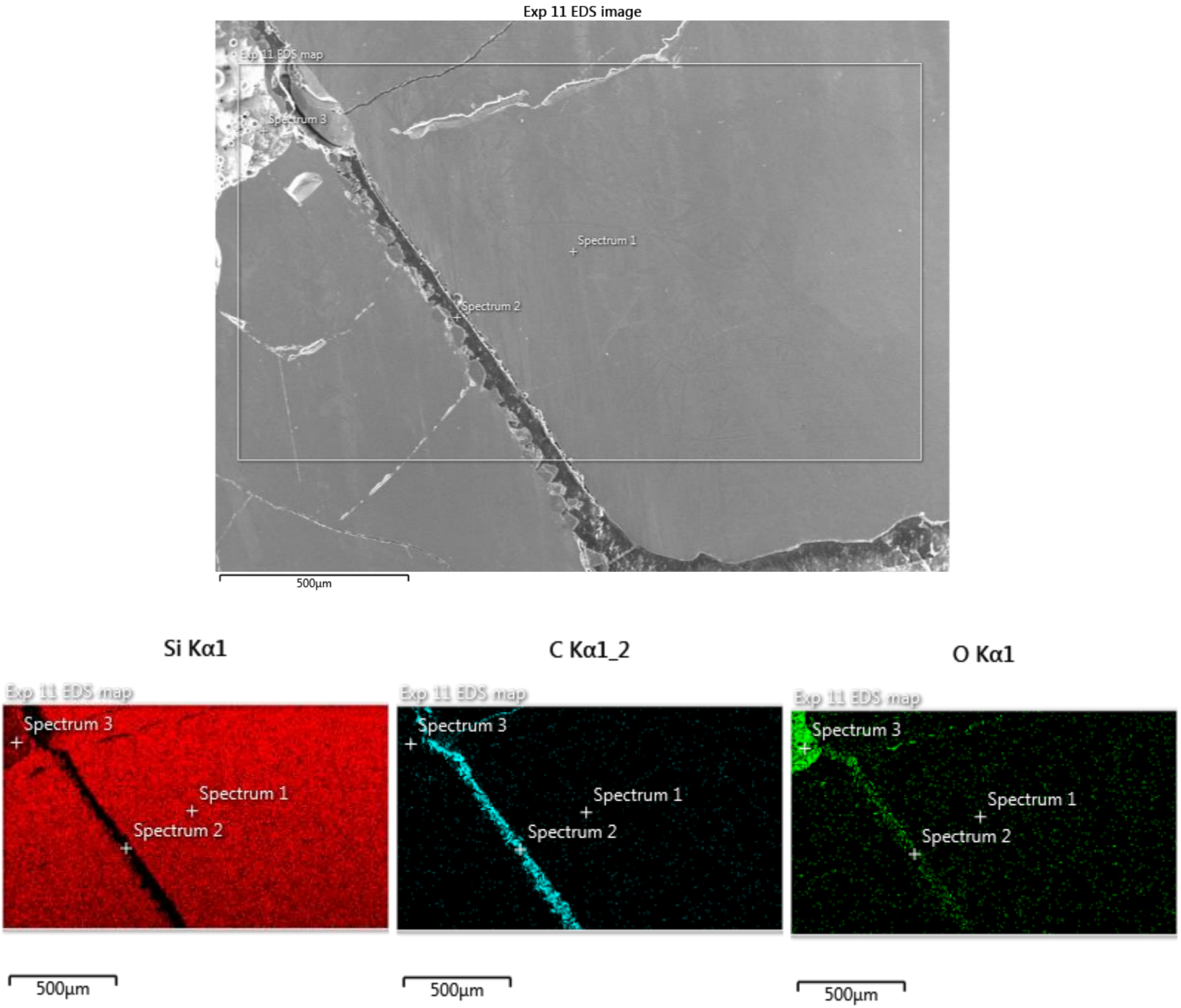

Figure 4.16: SEM and elemental X-ray mapping of experiment 11, taken at x65 magnification.

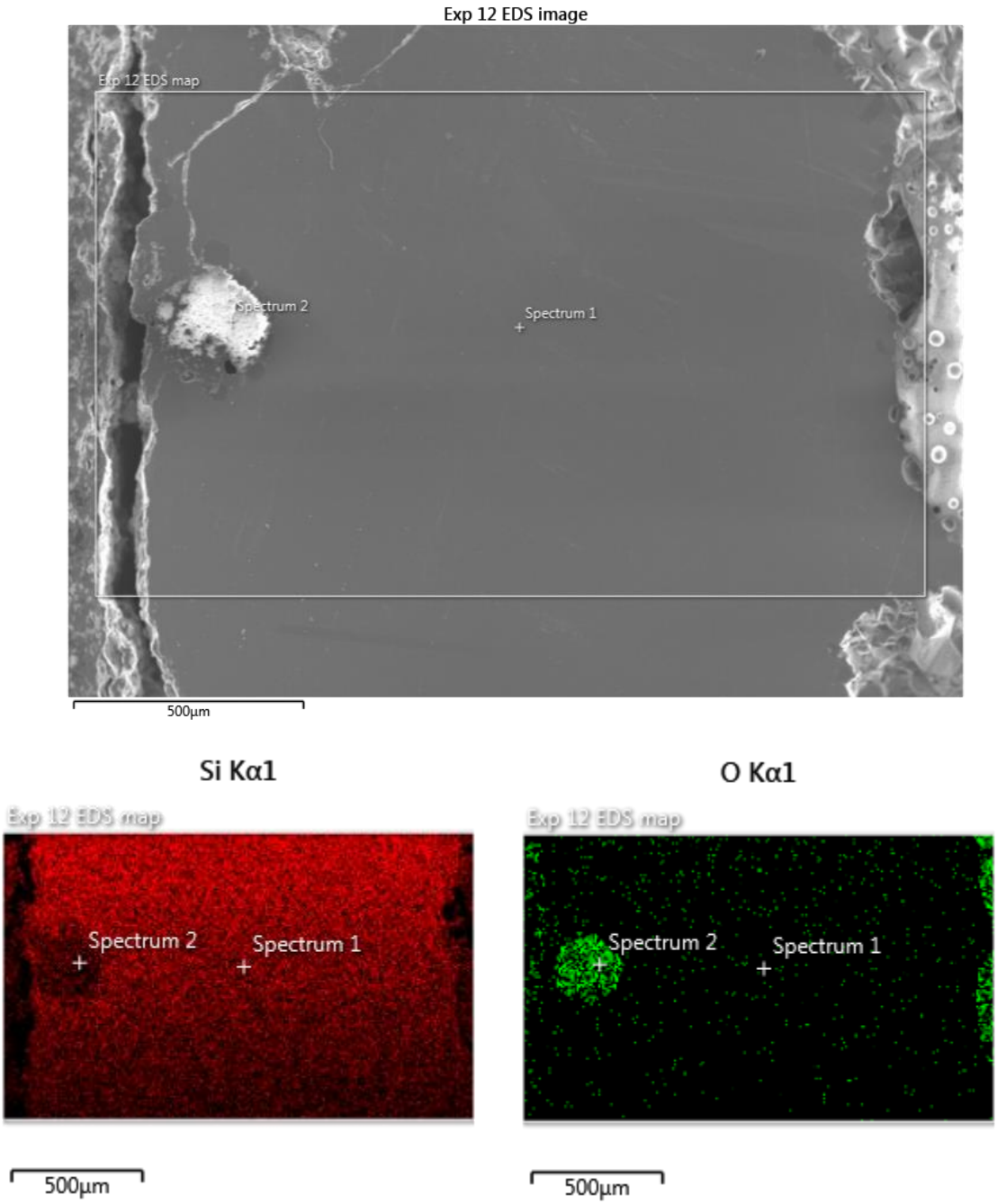

Figure 4.17: SEM and elemental X-ray mapping of experiment 12, taken at x65 magnification.

Table 4.5: The elemental compositions of each spectrum point from each sample.

Experiments	Spectrum 1 (wt%)	Spectrum 2 (wt%)	Spectrum 3 (wt%)
Experiment 1: No slag	Silicon: 96.32 Carbon: 3.68	Silicon: 55.96 Oxygen: 40.4 Carbon: 3.64	Silicon: 52.74 Oxygen: 47.26
Experiment 2: No slag	Silicon: 100	Silicon: 100	**X**
Experiment 3: CaO-SiO2	Silicon: 96.08 Carbon: 3.92	Silicon: 47.96 Carbon: 29.65 Oxygen 19.81 Aluminium: 0.78 Calcium: 1.8	Silicon: 38.87 Oxygen: 53.88 Calcium: 5.13 Aluminium: 2.12
Experiment 4: CaO-SiO2	Silicon: 94.99 Carbon: 4.47 Oxygen: 0.54	Carbon: 84.9 Oxygen: 14.29 Chlorine: 0.81	Carbon: 81.12 Oxygen: 17.98 Silicon: 0.26 Chlorine: 0.64
Experiment 5: CaO-SiO2	Silicon: 88.81 Carbon: 10.46 Oxygen: 10.46	Silicon:46.93 Oxygen: 36.97 Calcium:6.54 Carbon: 8.6 Aluminium:0.95	**X**
Experiment 6: CaO-SiO2	Silicon: 94.27 Carbon: 0.51 Oxygen: 0.51	Silicon: 27.33 Oxygen: 61.9 Carbon: 6.93 Calcium: 3.84	**X**
Experiment 7: FBR Si	Silicon: 97.16 Carbon: 2.84	Silicon: 46.1 Oxygen: 52.45 Aluminium: 1.45	**X**
Experiment 8: FBR Si	Silicon: 88.11 Carbon: 11.89	Silicon: 54.83 Oxygen: 43.57 Aluminium: 1.6	**X**
Experiment 9: FBR Si	Silicon: 94.01 Carbon: 5.25 Oxygen: 0.73	Silicon: 0.81 Carbon: 84.17 Oxygen: 14.06 Chlorine:0.96	Carbon: 86.11 Oxygen: 12.97 Chlorine: 0.92
Experiment 10: FBR Si	Silicon: 95.12 Carbon: 4.88	Silicon: 49.49 Oxygen: 50.50	Silicon: 2.03 Carbon: 77.7 Oxygen: 18.95 Chlorine: 1.32
Experiment 11: FBR Si	Silicon: 95.35 Carbon: 4.65	Silicon: 1.55 Carbon: 93.2 Oxygen 14.06 Chlorine: 1.18	Silicon: 50.67 Oxygen: 49.33
Experiment 12: FBR Si	Silicon: 93.7 Carbon: 5.83 Oxygen: 0.47	Silicon: 49.9 Oxygen: 45.71 Carbon: 4.39	**X**

4.4 Features and analysis of melted kerf samples

Figure 4.18 shows the 12 different crucibles containing the melted samples, cut, and polished, that were obtained from flux melting. The top row has experiments 1-6 in ascending order while the bottom row has experiments 7-12 in ascending order. Table 4.6 shows the GD-MS results for silicon kerf after it has undergone the entire refinement process. More detailed Figures of each sample can be found in appendix B.

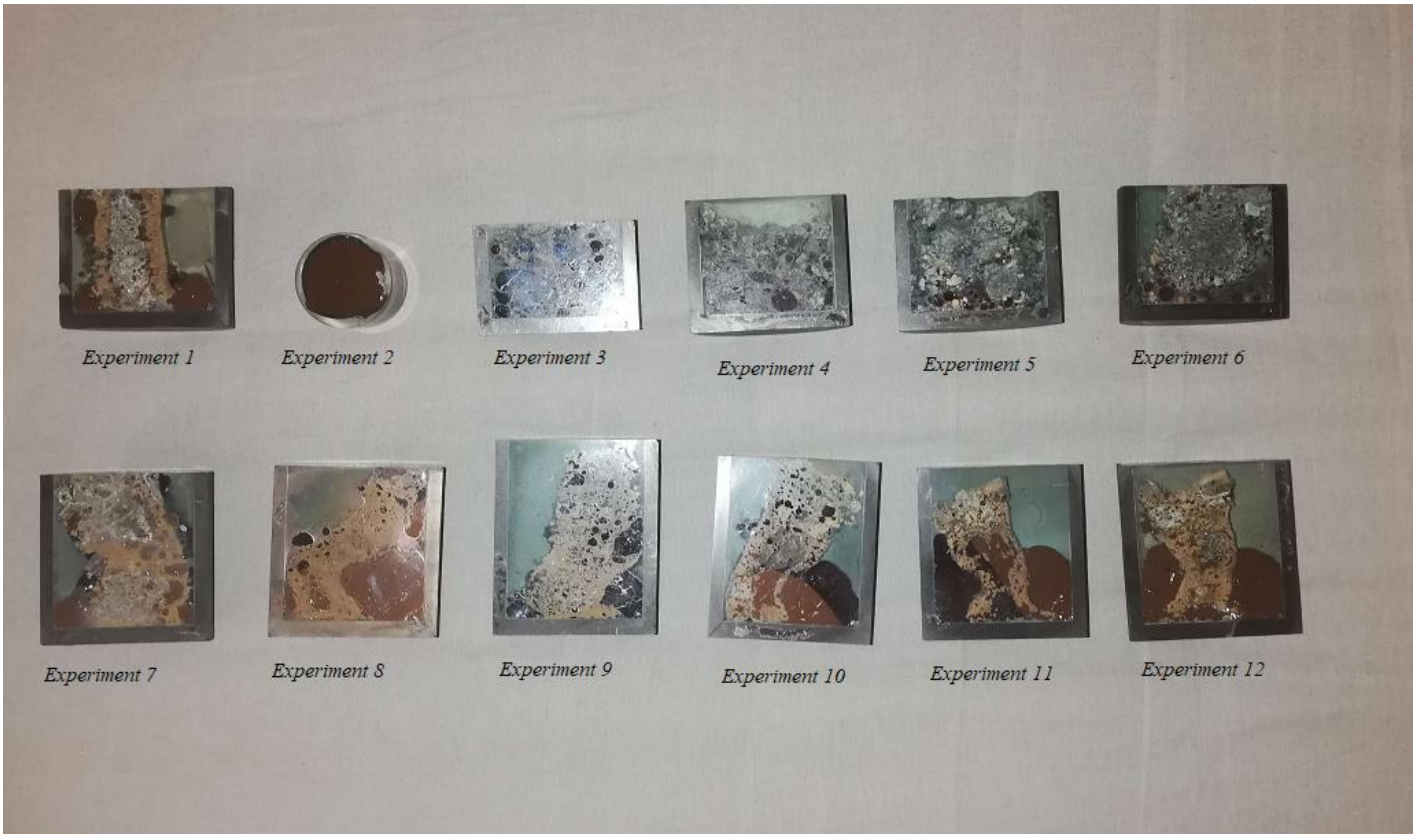

Figure 4.18: The 12 samples of silicon obtained from the furnace experiments.

Table 4.6: The GD-MS results for the silicon kerf after leaching and flux melting.

Element	**ppmw (parts per million by weight)**
Aluminium	100.5
Boron	0.14
Calcium	5.6
Copper	0.62
Iron	2.9
Gallium	0.35
Magnesium	0.27
Manganese	0.20
Nickel	8.8
Phosphorus	0.43
Titanium	0.32

5. Discussion

5.1 Leaching purification effect

Leaching, GD-MS, and ICP-MS were used to analyse and compare the silicon kerf, before and after the leaching process. From Figure 4.1 a SEM image that has been magnified by x50.00 shows the individual particles of silicon kerf before leaching with the white areas in the image, which are probably oxides. It was not possible to analyse as EDS cannot be used. Figure 4.3 shows a sample of silicon kerf magnified by x1.00k where the effects of the leaching can be seen. All the small holes and cracks located on the surface of the image are silicon particles that were removed during the polishing process. Both Figures 4.1 and 4.3 show that the Si-kerf material has Si particles with the sizes below 1 micron and a bit larger than 1 micron. From Figure 4.2, EDS analysis was used to map the elemental composition of the kerf before leaching. Trace amounts of oxygen, iron, nickel, and aluminium can be found within the silicon kerf sample. These elements are all impurities that need to be removed to produce SoG-Si. The EDS analysis for Figure 4.4 shows only 2 trace elements were found in abundance, carbon, and silicon in comparison to Figure 4.2 which had 5 trace elements found. While the EDS analysis shows that impurities were effectively removed during the leaching process, the amount of silicon that was found via EDS is also extremely low when comparing Figures 4.4 and 4.2. The most likely reason for this is a combination of a weak EDS signal that didn't pick up all the trace elements, the kerf powder being mixed with the epoxy and human error.

While the EDS analysis shows that impurities were removed from the leaching process, ICP-MS and GD-MS analysis allows for more accurate results. When comparing tables 4.1 and 4.2, elements such as aluminium, boron, chromium, copper, gallium, magnesium, nickel, titanium, and vanadium have a relatively similar ppmw, while elements such as calcium, iron, manganese, and phosphorus doesn't have as comparable a ppmw. While ICP-MS and GD-MS are both analytical techniques used for elemental analysis, they employ different principles and have distinct characteristics that can lead to variations in their results. For example, ICP-MS uses liquid samples while GD-MS uses solid samples. The different sample introduction methods can lead to variations in the types and amounts of elements detected. Another reason that could cause the difference in results between the ICP-MS and GD-MS is the detection sensitivity. ICP-MS is known for its high

sensitivity and ability to detect trace levels of elements, typically in the parts-per-billion (ppb) range. GDMS, on the other hand, can achieve lower detection limits in the parts-per-million (ppm) range. The difference in sensitivity can result in different detection capabilities for certain elements, leading to discrepancies in the measured concentrations. ICP-MS tests were also going to be used for silicon kerf samples after leaching, as well as for the HCl acid solution used in the leaching process, and silicon kerf samples after flux melting. However due to machine complications, only 1 ICP-MS test could be produced.

Table 4.3 shows the GD-MS results for the silicon kerf sample after leaching. By comparing table 4.2 with 4.3 we can see a reduction in certain elements and an increase in others. Aluminium was reduced by 38.18%, calcium was reduced by 14.24%, iron was reduced by 83.05%, gallium was reduced by 76.92%, manganese was reduced by 32%, nickel was reduced by75.8%, phosphorus was reduced by 73.46% and titanium was reduced by 41.07%. On the other hand, boron increased by 359.1%, chromium increased by 144.89%, magnesium increased by 22% and vanadium increased by 61.53%. During acid leaching, the main impurities that get reduced are aluminium, nickel, and iron. Boron and phosphorus are also important impurities that need to be reduced, but those impurities are removed during the melting process. So, impurities such as boron, phosphorus, magnesium, and chromium aren't expected to decrease after leaching, however the increase could be because of contamination that occurred during the handling or leaching of the silicon kerf.

5.2 Melting behaviour of Si-kerf

The experiments that were conducted using the IF75 furnace were not done in ascending order. 2 experiments could be conducted per day and experiments 2-4 were conducted first, followed by experiments 7-9. The following day experiments 10-12 were conducted followed by experiment 4-5 with the last experiment conducted being experiment 1 as that was the only experiment that would be heated for a duration of 2 hours. As seen in Figure 4.5, all experiments were conducted at stable temperatures and time. Experiments 1-6 were conducted at 1650°C while experiments 7-12 were conducted at 1600°C. The reasoning behind this was to compare the results of the different temperatures, but also since at 1650°C insures proper slag fluidity and a lower viscosity. The parameters of the experiment can be seen in table 4.4, and the reasoning behind the lower kerf and additive mass for experiments 5-6 is due to a lack of silicon kerf. Towards the end of the

experiments, around 50g of silicon kerf was missing so experiments 5-6 were carried out with the same weight percentages as originally planned, only with different masses. The weight loss from each experiment can be seen in table 5.1. Experiments 1-2 have a weight loss of around 13%, experiments 3-4 have a weight loss of around 15%, experiments 5-6 have a weight loss of around 6% while experiments 7-12 have a weight loss of around 7%.

From Figure 4.18, all the silicon from each sample formed towards the bottom of the crucible, while all the SiC, SiO_2 and oxidation occurred towards the top of the crucible. This is because the main crucible that was used as shown in Figure 3.4 is much larger than the 3 crucibles within it. This means that the temperature towards the bottom of the crucible was a lot higher than the temperature towards the top of the crucible. This difference in temperature allowed pure silicon to form towards the bottom of the crucible while the lower temperature towards the top of the crucible allowed for more oxidation and the formation of SiC and SiO_2.

The general loss of material for all 12 samples can be attributed to a combination of multiple things. The loss of hydrocarbons, polymer carbons and SiO gas is lost during the melting process. The formation of SiO may be due to reaction (13) in which the surface oxide of SiO_2 on Si grain reacts with the Si core:

$$SiO_2 + Si = 2SiO(g) \qquad (13)$$

As seen in table 5.1, experiments 1-2 were expected to have higher amounts of weight loss as no additives were added. For experiments 3-6 it was expected to have a lower weight loss due to the addition of CaO-SiO_2 slag. Experiments 3-4 have comparable percentage weight loss to experiments 1-2. This is because the amount of CaO-SiO_2 wasn't enough to make a difference. Experiments 5-6 are more in line with expectations. Experiments 7-12 also were expected to have lower percentage weight losses. The additive for these experiments was FBR Si which assisted in the melting process and combined with the liquid silicon. For each experiment less kerf powder was also added meaning less overall mass loss due to the decrease in silicon kerf and an increase in FBR Si granules.

Table 5.1: The percentage weight loss of the samples after flux melting.

Experiments	Weight loss in %
Experiment 1: No slag	13.22
Experiment 2: No slag	13.54
Experiment 3: CaO-SiO_2	14.83
Experiment 4: CaO-SiO_2	15.80
Experiment 5: CaO-SiO_2	7.59
Experiment 6: CaO-SiO_2	5.53
Experiment 7: FBR Si	9.67
Experiment 8: FBR Si	4.19
Experiment 9: FBR Si	8.06
Experiment 10: FBR Si	9.35
Experiment 11: FBR Si	7.09
Experiment 12: FBR Si	7.09

5.3 Microstructural analysis

5.3.1 Si-kerf melting

Experiments 1 and 2 melted in the furnace without the addition of any additives. Experiment 1 was heated for a duration of 120 minutes while experiment 2 was heated for a duration of 60 mins. From Figure 4.6 the different spectrum points can be seen. Spectrum 1 as marked in the Figure is the formation of pure silicon as it is 96.32% silicon. Spectrum 2 is the formation of SiO_2 due to oxidation of silicon during the melting process. Spectrum 3, which is recognized by its white appearance in the SEM image, is another point where SiO_2 formed due to oxidation. The 3.68% carbon that was found in spectrum 1 is most likely due to contamination of the sample, either while handling the sample or contamination within the SEM machine that affected the microscope. The EDS mapping also shows which elements are most present and silicon and oxygen are the most present elements. This makes sense as there are no additives to help with the melting process. All

the oxygen that can be found surrounding the large silicon granules point towards SiO_2 phase. Experiment 2 is slightly different as it was not cut from the crucible. Due to unseen circumstances, the sample from experiment 2 became loose and rather than pouring epoxy inside the crucible and cutting the crucible, a large chunk of silicon was in cased in epoxy and polished instead. This is the reasoning behind the difference in SEM imagery and why silicon was the only trace element found during EDS analysis. Just like the leached mounted sample that produced poor EDS results for experiment 2, the most likely reason that experiment 2 produced poor results is also a combination of a weak EDS signal, the epoxy coating and human error.

5.3.2 CaO-SiO_2 slag use

Experiments 3-6 were melted in the furnace along with CaO-SiO_2 slag. All 4 experiments were heated for the same duration of 60 minutes, however, experiments 5 and 6 conducted with less kerf and slag, but with the same weight ratio due to a lack of 50g kerf. The addition of CaO-SiO_2 slag was added to assist in deoxidation and desiliconization. As can be seen from Figure 4.18 and Figures X from appendix B, experiments 3 and 4 produced a sufficient amount of pure silicon while experiments 5 and 6 produced a lot less in comparison. While oxidation affected these samples like all other samples, the difference in kerf mass and slag mass also attributed to less silicon being formed in experiments 5 and 6. The more slag that is added to the silicon can attribute to larger loss in mass as can be seen in reaction (14).

$$(SiO_2) + C = SiO(g) + CO(g) \qquad (14)$$

From table 4.5 the data from the spectrum points can be seen. For experiments 3-6, pure silicon can be found within each sample at spectrum point 1 having trace amounts of oxygen and carbon. This carbon is most likely the same contamination that occurred in experiments 1-2. The contamination most likely occurred either while handling the sample or was contamination that was present within the SEM microscope during SEM analysis. Spectrum points 2 and 3 for experiment 3 point towards it being the formation of SiC as the morphology and colour are similar to SiC and not SiO_2. The point analysis data also points towards these spectrum's being SiC. For experiment 4, spectrum points 2 and 3 had high amounts of carbon and oxygen. This is most likely due to the SEM imagery being taken near the graphite crucible wall which is the only source of

carbon besides small trace amounts within the sample. For experiment 5, spectrum point 2 indicates a formation of SiO_2 while spectrum point 2 for experiment 6 indicates a formation of Silica.

5.3.3 FBR Si use

Experiments 7-12 melted in the furnace along with the addition of FBR Si. All 6 experiments were heated for the same duration of 60 minutes. The addition of FBR Si was used to help with the assisting of melting the kerf powder. Fine Si powders with surface oxide layer do not melt as well as large solid particle in a furnace and with the addition of FBR Si which is a pure silicon, the melting process is improved. This improvement in the melting process can be seen in Figure 4.18. The FBR Si samples produced the highest quantity and quality of silicon after the entire refinement process. Oxidation was a problem just as it was for all the other samples and the effects of oxidation can visibly be seen in Figure 4.18 and Figures from appendix X, but the FBR Si granules there were added to assist with the melting were heavy enough to sink to the bottom of the crucible which resulted in larger lumpy silicon particles being formed after melting. From table 4.5 the data from the spectrum points can be seen. For spectrum point 1 for experiments 7-12, pure silicon can be found with each sample having trace amounts of carbon. This carbon is a result of the same contamination that affected experiments 1-6 and occurred either during the handling of the sample or contamination within the SEM microscope. For spectrum point 2, experiments 7,8,10 and 12 indicate the formation of SiO_2, while experiments 9 and 11 points toward the SEM imagery picking up on the carbon from the graphite crucible wall. For spectrum point 3, experiments 10 points towards SEM imagery picking up on the carbon from the crucible yet again, while experiment 11 points towards the formation of SiO_2.

5.4 Comparing the melting processes

Experiments 7-12 produced the best results overall, both in terms of quality and quantity of silicon found as the FBR Si additives assisted in both melting and production of silicon. Experiments 1-4 produced the second-best results while experiments 5-6 produced the worst results of all 12 samples. Due to a combination of the temperature used and the oxidation that occurred during the melting process, pure silicon was only produced in smaller amounts than anticipated as can be seen from Figure 4.18 and Figures from appendix B along with larger quantities of SiO_2 and SiC.

According to information given by REC Solar Norway, SoG-Si needs to have the following specifications.

- Boron < 80 ppbw
- Phosphorus < 300 ppbw
- C < 5 ppmw
- Total surface metals (iron, chromium, nickel, zinc) < 50 ppbw
- Bulk total metals (iron, chromium, nickel, copper, zinc, aluminium) < 15ppbw

The final GD-MS results from table 4.6 show that many of these requirements have been achieved. Both the boron, phosphorus, total surface metals and bulk total metals have been purified to the point where the requirements for SoG-Si have been fulfilled. Overall aluminum was reduced by 99.09%, boron was reduced by 68.18%, calcium was reduced by 85.22%, copper was reduced by 70.47%, iron was reduced by 98.51%, gallium was reduced by 93.26%, magnesium was reduced by 94.6%, manganese was reduced by 92%, nickel was reduced by 94.81%, phosphorus was reduced by 95.61% and titanium was reduced by 94.28%. While these results are great and the numbers point towards the kerf being refined into SoG-Si, the silicon that was produced needs to go through an additional refinement process to be considered SoG-Si. By putting the silicon through an additional step of refinement such as directional solidification, the silicon could then be refined and classified as SoG-Si. In addition to an additional refinement step, the leaching and melting process would need to be further optimized to remove more impurities during the leaching and melting stage of the refinement process.

6. Conclusion

The results from the refinement process were very promising and aligned with the theoretical aspects of this experiment. However due to some unexpected circumstances such as a vacuum sealed furnace not being available for use and the ICP-MS machine needing to be recalibrated and not being able to provide the analysis needed, contributed to slightly different results than expected. The main conclusions of this thesis can be summarized as:

- The leaching process went as expected as leaching was used primarily for the removal of metallic impurities and the acid leaching was capable of removing impurities found within the kerf.
- Si-kerf melting did not produce a large amount of silicon due to using an open top induction furnace, and Ar purging over the crucible containing material. However, the method works and can be optimized by increasing the temperature used to melt the silicon. As discussed earlier in chapter 2.1.2, silicon is usually heated in an arc furnace at a temperature of 1900°C -2000°C. By increasing the temperature from 1600°C -1650°C to 1700°C or 1800°C, the resulting temperature increase will remove oxidation faster and allow for more silicon to be produced.
- The ICP-MS and GD-MS analysis also proved to be vital in analysing the samples as it showed how effective the leaching and melting processes were.
- The best results turned out to be the FBR Si addition to Si-kerf and melting, followed by the $CaO\text{-}SiO_2$ slag experiments and then finally the no additive experiments.
- While the GD-MS results were promising and there was a great deal of reduction in impurities, which pointed towards the necessary impurity levels to be considered SoG-Si, the silicon needs to go through an additional refinement process like directional solidification.
- Overall, the theory and experimental procedure used for producing silicon was found to be effective, however with some slight adjustments in the refinement process, SoG-Si could be produced.

References

[1] Press release, "Renewable electricity growth is accelerating faster than ever worldwide, supporting the emergence of the new global energy economy," IEA - International Energy Agency, 2021 December 2021. [Online]. Available: https://www.iea.org/news/renewable-electricity-growth-is-accelerating-faster-than-ever-worldwide-supporting-the-emergence-of-the-new-global-energy-economy.

[2] "Renewable electricity growth is accelerating faster than ever worldwide, supporting the emergence of the new global energy economy," IEA - International Energy Agency, September 2022. [Online]. Available: https://www.iea.org/reports/solar-pv.

[3] A. L. H. Z. P. C. G. Khadidja Hachichi, "Silicon Recovery from Kerf Slurry Waste: a Review of Current Status and Perspective," 2018.

[4] D. Verdu, "Ny ESS prosess basert på wafer fines(kerf) som råvare," Enova, 2019. [Online]. Available: https://www.enova.no/om-enova/om-organisasjonen/teknologiportefoljen/ny-ess-prosess-basert-pa-wafer-fineskerf-som-ravare/.

[5] "Periodic Table - Silicon," Royal Society of Chemistry, [Online]. Available: https://www.rsc.org/periodic-table/element/14/silicon.

[6] "Solar Photovoltaic Cell basics," Office of Energy Effeiciency and Renewable Energy, [Online]. Available: https://www.energy.gov/eere/solar/solar-photovoltaic-cell-basics.

[7] "Our Process," Mississippi Silicon, [Online]. Available: https://www.missilicon.com/process.

[8] A. S. J. K. T. Halvard Tveit, "Production of High Silicon Alloys," 1997.

[9] M. Tangstad, Metal production in Norway, Akademika, 2013.

[10] G. T. M. T. Jafar Safarian, "Processfor Upgrading Metallurigcal Grade Silicon to Solar Grade Silicon," 2012.

[11] J. Bernreuter, "Polysilicon Production Processes," Bernreuter Research, 29 June 2020. [Online]. Available: https://www.bernreuter.com/polysilicon/production-processes/.

[12] "Leaching," Britannica, [Online]. Available: https://www.britannica.com/science/metallurgy/Forging.

[13] M. Zhu, "Siliicon purification by acid leaching and slag refining techniques," NTNU, 2021.

[14] J. S. a. S. Espelien, "Effect of acid leaching conditions on impurity removal from silicon," AIMS Energy, 2017.

[15] "Technology," REC silicon, [Online]. Available: https://recsilicon.com/technology/.

[16] "Periodic table - Argon," Royal Society of Chemistry, [Online]. Available: https://www.rsc.org/periodic-table/element/18/argon.

[17] R. S. C. C. Y. G. S. J. l. M. R. M. D. S. Kryzstof Adamcyzk, "Recombination Strength of Dislocations in High-Performance Multicrystalline/Quasi-Mono Hybrid Wafers During Solar Cell Processing," 2017.

[18] L. Z. L. D. Anping Dong, "Beneficial and Technological Analysis for the Recycling of Solar Grade Silicon Wastes," Journal of the minterals, metals and materials society, 2011.

[19] Osaka Fuji Corporation, "Slicing process," Osaka Fuji Corporation, [Online]. Available: https://www.ofic.co.jp/en/r_and_d/slicing/.

[20] J. Marsh, "What are the different types of solar panels?," Energysage, 23 january 2023. [Online]. Available: https://news.energysage.com/types-of-solar-panels/.

[21] Fraunhofer Institute for Solar Energy Systems, , "Photovoltaics Report," 2023.

[22] "Scanning electron microscope (SEM)," MicroscopeWiki, 6 October 2022. [Online]. Available: https://microscopewiki.com/scanning-electron-microscope/.

[23] "Glow Discharge Mass Spectrometry (GDMS) Analysis," Goverment of Canada, [Online]. Available: https://nrc.canada.ca/en/research-development/products-services/technical-advisory-services/glow-discharge-mass-spectrometry-gdms-analysis.

[24] Y. H. J. R. S. Michael D. Gaslock, "Inductively Coupled Plasma Mass Spectrometry," ScienceDirect, [Online]. Available: https://www.sciencedirect.com/topics/materials-science/inductively-coupled-plasma-mass-spectrometry.

[25] Bloomberg News, "Silicon’s 300% surge throws another price shock at the world," Mining.com, 1 October 2021. [Online]. Available: https://www.mining.com/web/silicons-300-surge-throws-another-price-shock-at-the-world/.

[26] M. Kadkhodabeigi, "Modeling of tapping processes in submerged arc furnaces," 2021.

[27] "Glow Discharge Mass Spectrometry : GDMS," Toray Research, [Online]. Available: https://www.toray-research.co.jp/en/technicaldata/techniques/GDMS.html.

[28] R. A. Richard Gilstrap, "A colloidal nanoparticle form of indium tin oxide: system development and characterization," 2009.

Appendix

Appendix A: Sample imagery

Appendix B: Risk assessment

Appendix A: Sample imagery

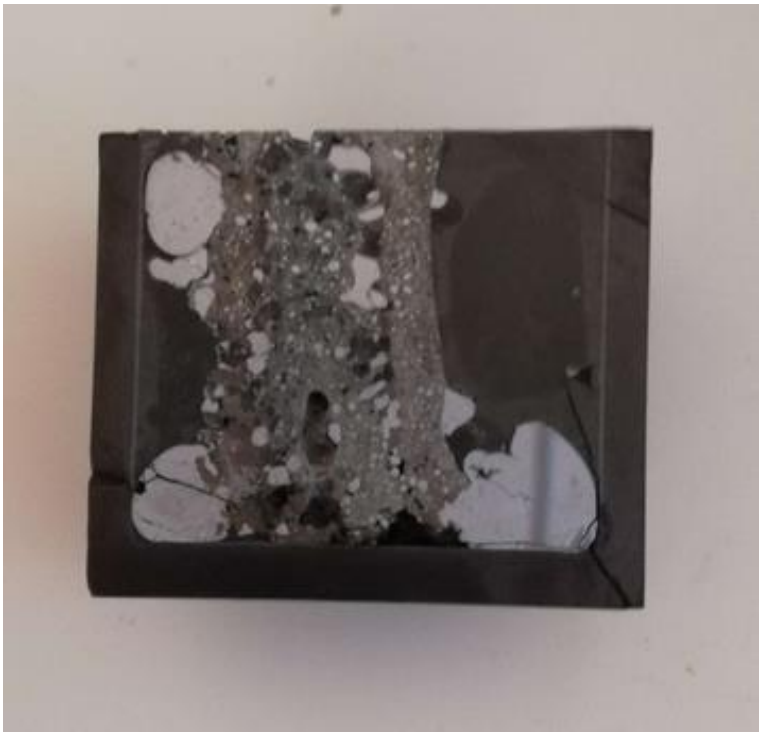

Figure 1A: Experiment 1

Figure 2A: Experiment 2

Appendix A: Sample imagery

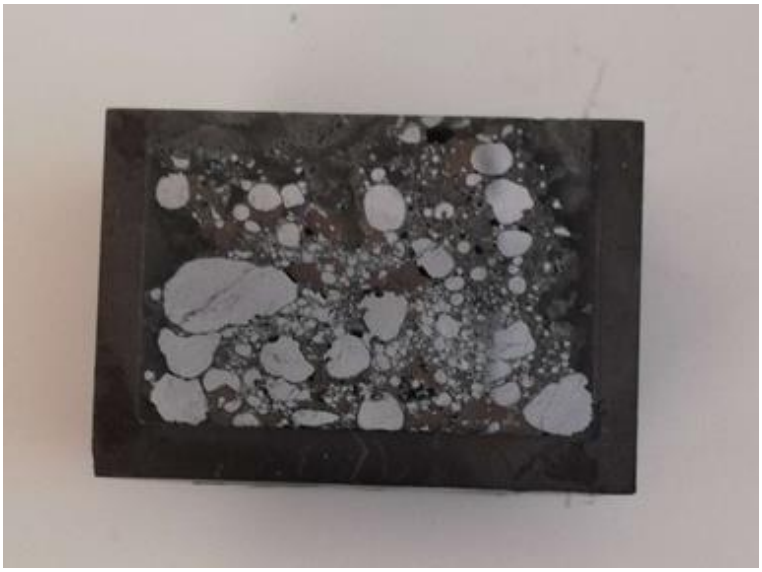

Figure 3A: Experiment 3

Figure 4A: Experiment 4

Appendix A: Sample imagery

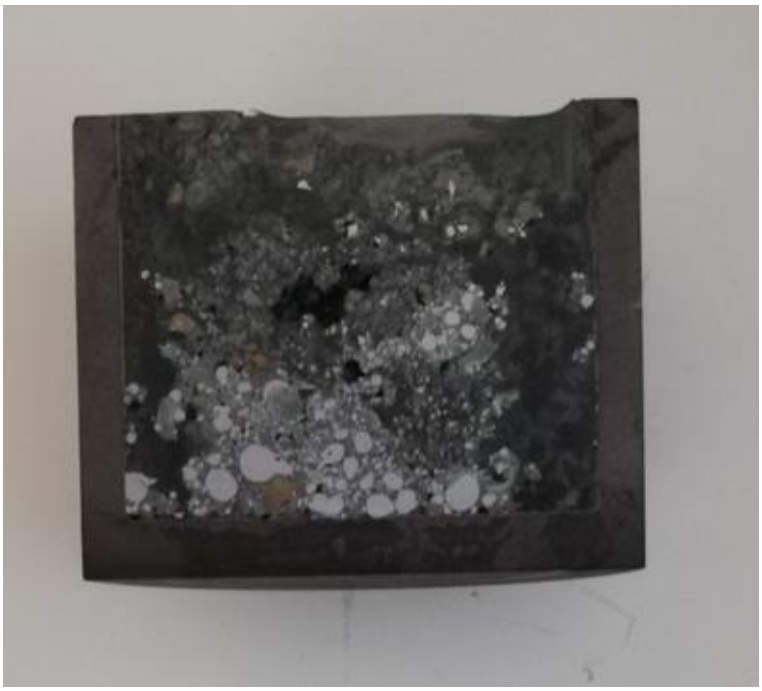

Figure 5A: Experiment 5

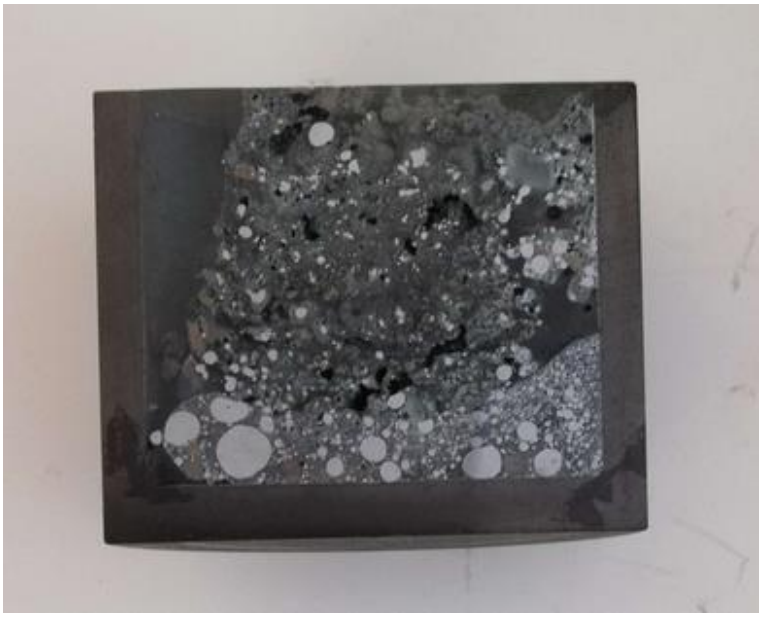

Figure 6A: Experiment 6

Appendix A: Sample imagery

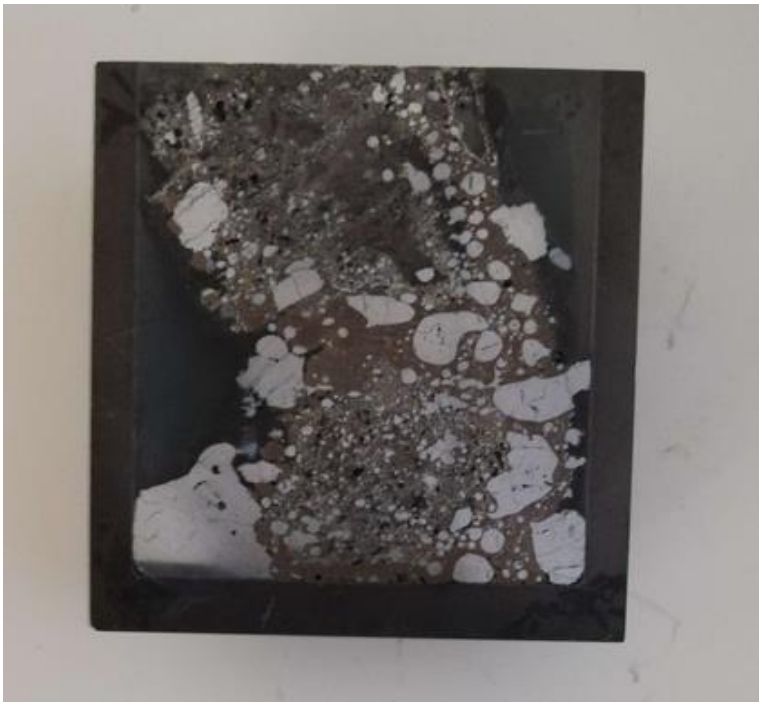

Figure 7A: Experiment 7

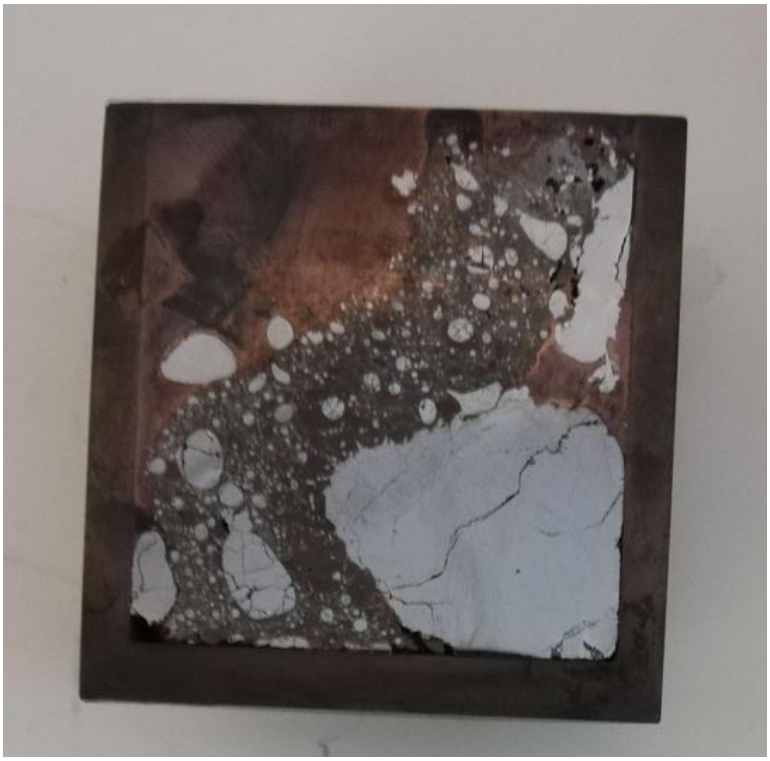

Figure 8A: Experiment 8

Appendix A: Sample imagery

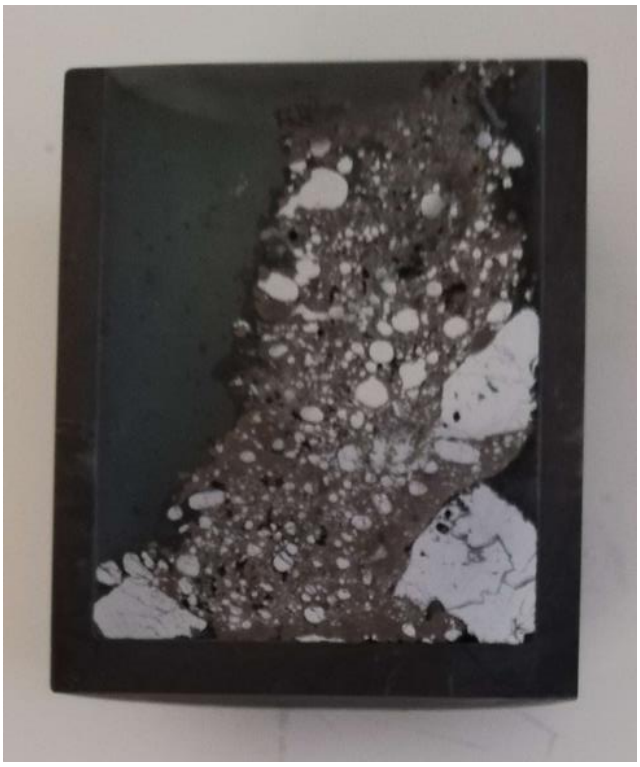

Figure 8A: Experiment 8

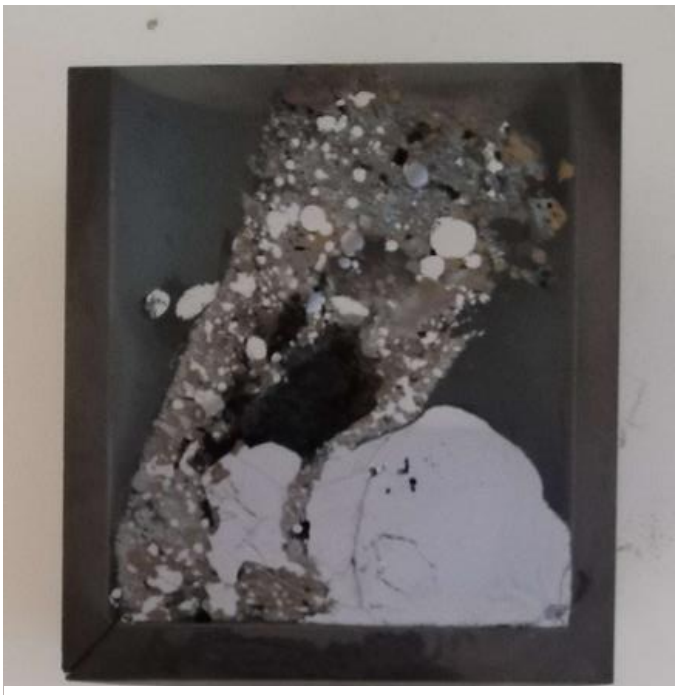

Figure 10A: Experiment 10

Appendix A: Sample imagery

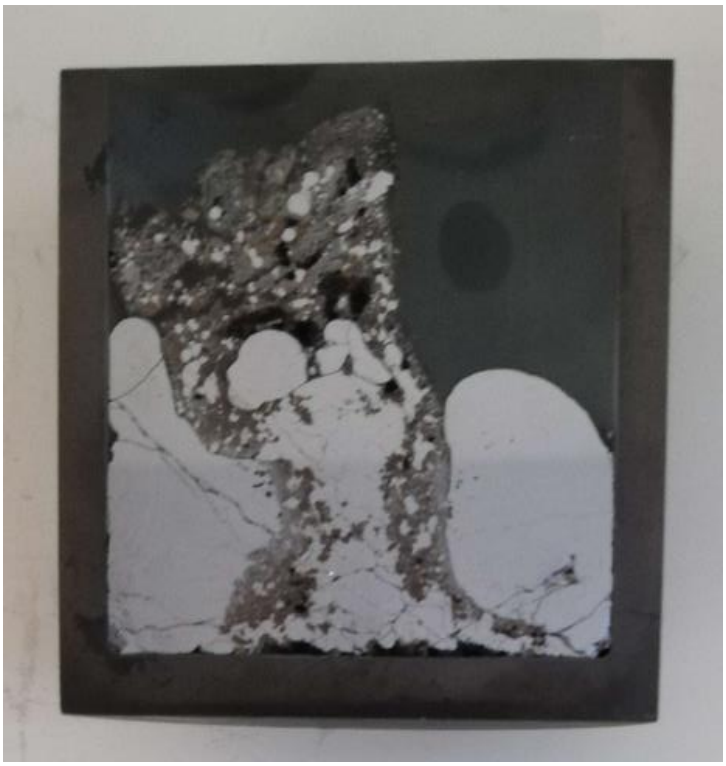

Figure 11A: Experiment 11

Figure 12A: Experiment 12

Appendix B: Risk assessment

Aktivitet/arbeidsoppgave	Mulig uønsket hendelse	Eksisterende risikoreduserende tiltak	Vurdering av sannsynlighet (S)	Vurdering av konsekvens (K) *Vurder en konsevenskategori om gangen. Menneske skal alltid vurderes.*				Risikoverdi (S x K)	Forslag til forebyggende og/eller korrigendene tiltak *Prioriter tiltak som kan forhindre at hendelsen inntreffer (sannsynlighetsreduserende tiltak) foran skjerpet beredskap (konsekvensreduserende tiltak)*	Restrisiko etter tiltak (S x K)
			(1-5)	Menneske (1-5)	Øk/materiell (1-5)	Ytre miljø (1-5)	Omdømme (1-5)			
Smelting of material	Water leackage in the furnace and contact with hot crucible		*1*	*2*	*1*	*1*	*1*	*2*	*Use safety glasses, monitor the furnace during the work, if any explotion due to water leackage the power is turned off and room responsible is informed.*	3
Smelting of material	Inhaling gasses during initial heati	Masks and ventilation tube	1	2	1	2	1	2	Use the ventilation tube directly over the furnace and when going close to the furnace, use the mask until temperature has reached 1500	1
Smelting of material	Inhaling dust during furnace cleanir	safety glasses, mask, gloves, proper clothing	2	2	1	1	4	4	use protective equipment correctly, coordinated, calm movements. Follow the instructions. Ventilation is on during cleaning. Vacuum	3
Smelting of material	Spillage of heated material	safetly glasses, glovees, proper clothing	1	4	1	2	2	2	3 smaller crucibles with the material will be contained within a larger crucible with a lid. This will prevent any form of major spillage.	1
smelting of material	burns	safety glasses, mask, gloves, proper cloths	1	3	1	1	1	3	Material will not be handled until after 2-3 hours cooling period. Use proper safety equipment while handling material.	2
Crucible crushin/cutting	particle in eyes/irritation	safety glasses, mask, gloves, proper cloths	1	3	2	2	3	3	Follow the procedures, if hammer is used the material must be crushed in plastic bags	3
weighing of materials	inhaling dust	safety glasses, mask, gloves, proper cloths	2	1	1	1	1	2	work under deduction and use mask if needed	1
Charging of crucible	inhaling dust	safety glasses, mask, gloves, proper cloths	2	1	1	1	1	2	use protective equipment correctly, coordinated, calm movements. Follow the instructions. Ventilation is on during cleaning. Vacuum cleaner use.	1
Mixing the Si/slag powders	inhaling dust	safety glasses, mask, gloves, proper cloths	2	1	1	1	2	2	use protective equipment correctly, coordinated, calm movements. Follow the instructions. Ventilation is on during cleaning. Vacuum cleaner use.	1
Leaching and solution prepar	acid contact with skin, inhaling gase	safety glasses, mask, gloves, proper cloths	4	2	1	1	2	3	Everything is performed in fume hood, instructions for acid uses and dilution of acids will be followed. The work will be communicated with the technicians and supervisors.	1
Drying samples	Skin burn	Gloves use	2	1	1	1	1	2	The standard procedures will be followed.	
Milling	inhaling dust	safety glasses, mask, gloves, proper cloths	2	1	1	1	1	2	use protective equipment correctly, coordinated, calm movements. Follow the instructions. Ventilation is moved close to the mill chamber, when it is opened carfully. Ventilation must not suck the powder ou.	1
SEM sample preparation	Inhaling gases when sample is prep	safety glasses, mask, gloves, proper cloths	1	1	1	1	1	2	In fume hood. And follow the general metallugraphy lab instructions	2

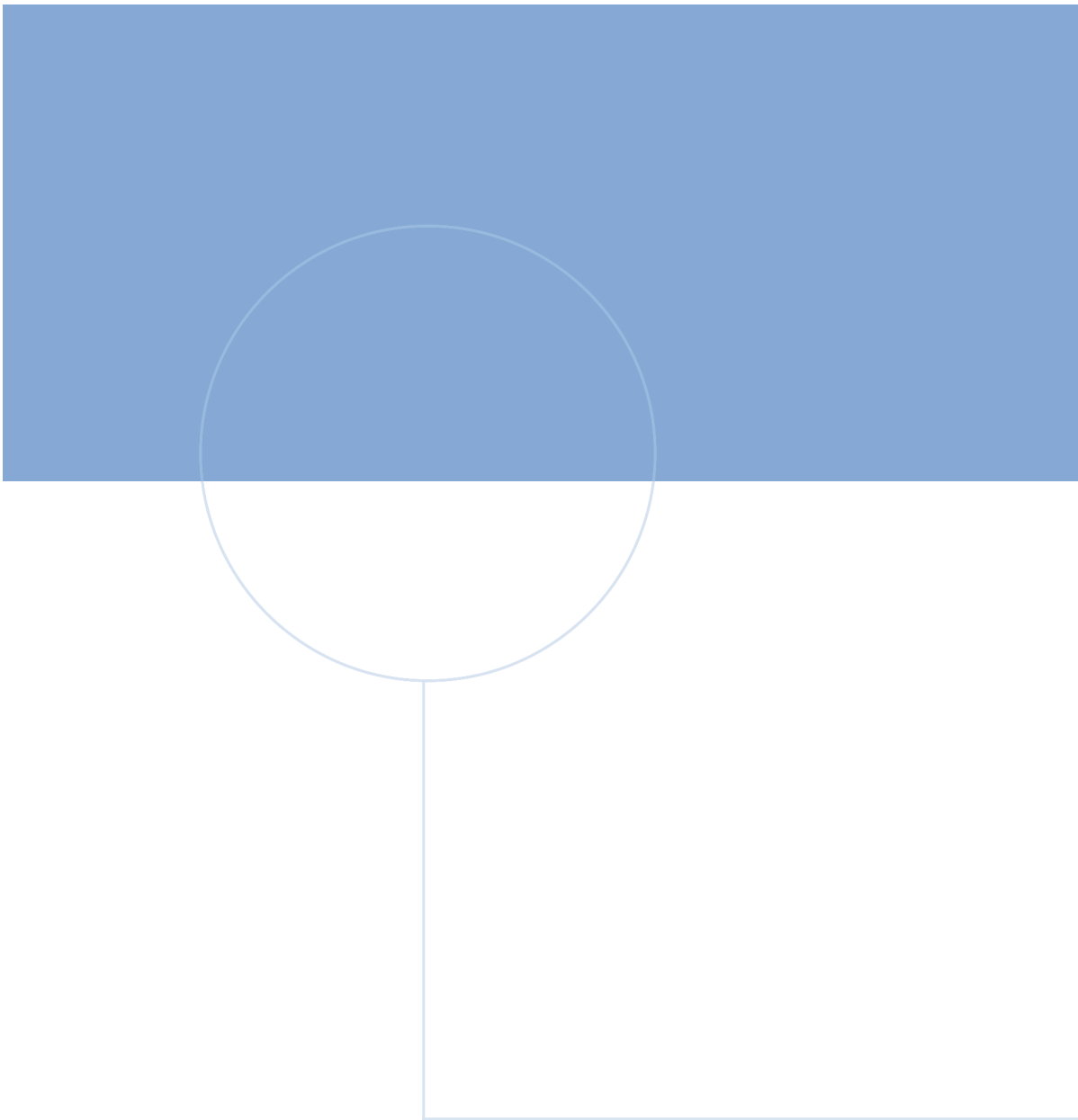

NTNU

Norwegian University of
Science and Technology